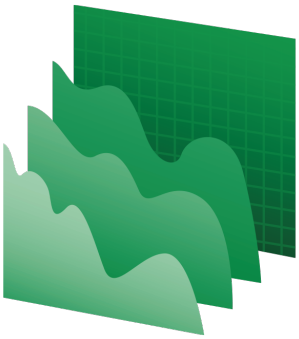

In Situ database Analyses Report

TSG

prepared by the Pi-MEP Consortium

October 15, 2018

Contents

Acronym

Aquarius	NASA/CONAE Salinity mission
ASCAT	Advanced Scatterometer
BLT	Barrier Layer Thickness
CMORPH	CPC MORPHing technique
CTD	Instrument used to measure the conductivity, temperature, and pressure of seawater
DM	Delayed Mode
EO	Earth Observation
ESA	European Space Agency
FTP	File Transfer Protocol
GOSUD	Global Ocean Surface Underway Data
GTMBA	The Global Tropical Moored Buoy Array
Ifremer	Institut français de recherche pour l'exploitation de la mer
IPEV	Institut polaire français Paul-Émile Victor
ISAS	In Situ Analysis System
L2	Level 2
LEGOS	Laboratoire d'Etudes en Géophysique et Océanographie Spatiales
LOCEAN	Laboratoire d'Océanographie et du Climat : Expérimentations et Approches Numériques
LOPS	Laboratoire d'Océanographie Physique et Spatiale
MEOP	Marine Mammals Exploring the Oceans Pole to Pole
MLD	Mixed Layer Depth
NRT	Near Real Time
Pi-MEP	Pilot Mission Exploitation Platform
PIRATA	Prediction and Researched Moored Array in the Atlantic
QC	Quality control
RAMA	Research Moored Array for African-Asian-Australian Monsoon Analysis and Prediction
RR	Rain rate
SAMOS	Shipboard Automated Meteorological and Oceanographic System
SMAP	Soil Moisture Active Passive (NASA mission)
SMOS	Soil Moisture and Ocean Salinity (ESA mission)
SSS	Sea Surface Salinity
SST	Sea Surface Temperature
STD	Standard deviation
Survostral	SURVeillance de l'Océan AuSTRAL (Monitoring the Southern Ocean)
TAO	Tropical Atmosphere Ocean
TSG	Thermosalinograph

1 Overview

This report presents some characteristics of the TSG in situ dataset used by the Pi-MEP to validate SMOS, SMAP and Aquarius satellite SSS products. A series of plots is proposed showing:

- Number of SSS data as a function of time and distance to coast
- Histogram of shallowest salinity and pressure (if relevant)

- Temporal mean of shallowest salinity and pressure (if relevant)
- Temporal STD of shallowest salinity
- Spatial density of shallowest salinity
- ΔSSS between local in situ data and ISAS analyses sorted as function of geophysical conditions
- Conditional analyses

The conditional analyses proposed in the document, correspond to filter/subdivide the in situ dataset following specific geophysical conditions:

- **C1**:if the local value at in situ location of estimated rain rate is high (ie. $>$ 10 mm/h) and mean daily wind is low (ie. $<$ 5 m/s).
- **C2**:if the prior 10-days history of the rain and wind at in situ location show high (ie.$>$ 5 mm/h) and low (ie.$<$ 5 m/s) median values, respectively.
- **C3**:if both C1 and C2 are met.
- **C4**:if the mixed layer is shallow with depth <20m.
- **C5**:if there is a barrier layer with thickness $>$ 10 m.
- **C6**:if the in situ data is located where the climatological sss standard deviation is high (ie. above $>$ 0.2).

For each conditions, the temporal mean (gridded over spatial boxes of size 1°x1°) and the histogram of the difference ΔSSS between ISAS and in situ SSS value are presented.

1.1 In situ dataset

1.1.1 TSG

The TSG dataset is subdivided into 6 subdatasets following TSG data providers subdivisions:

- LEGOS-DM:
  The TSG-LEGOS-DM dataset correspond to sea surface salinity delayed mode data derived from voluntary observing ships collected, validated, archived, and made freely available by the French Sea Surface Salinity Observation Service (Alory et al. (2015)). Adjusted values when available and only collected TSG data that exhibit quality flags=1 and 2 were used.
- GOSUD-Research-vessel:
  The TSG-GOSUD-Research-vessel dataset correspond to French research vessels that have been collecting thermo-salinometer (TSG) data since the early 2000 in contribution to the GOSUD program. The set of homogeneous instruments is permanently monitored and regularly calibrated. Water samples are taken on a daily basis by the crew and later analysed in the laboratory. The careful calibration and instrument maintenance, complemented with a rigorous adjustment on water samples lead to reach an accuracy of a few 10^{-2} PSS in salinity. This delayed mode dataset (Gaillard et al. (2015)) is updated annually and freely available here. Adjusted values when available and only collected TSG data that exhibit quality flags=1 and 2 were used.

- GOSUD-Sailing-ship: The TSG-GOSUD-Sailing-ship dataset correspond to Observations of Sea surface salinity obtained from voluntary sailing ships using medium or small size sensors. They complement the networks installed on research vessels or commercial ships. This delayed mode dataset (Reynaud et al. (2015)) is updated annually as a contribution to GOSUD (http://www.gosud.org) and freely available here. Adjusted values when available and only collected TSG data that exhibit quality flags=1 and 2 were used.

- SAMOS: The TSG-SAMOS dataset correspond to "Research" quality data from the US Shipboard Automated Meteorological and Oceanographic System (SAMOS) initiative (Smith et al. (2009)). Data are available at http://samos.coaps.fsu.edu/html/. Adjusted values when available and only collected TSG data that exhibit quality flags=1 and 2 were used.

- LEGOS-Survostral: The TSG-LEGOS-Survostral dataset correspond to delayed mode regional data from TSG installed on the Astrolabe vessel (IPEV) during the round trips between Hobart (Tasmania) and the French Antarctic base at Dumont d'Urville (Morrow and Kestenare (2014)). It is provided by the Survostral project and available via ftp. Adjusted values when available and only collected TSG data that exhibit quality flags=1 and 2 were used.

- LEGOS-Survostral-Adélie: The TSG-LEGOS-Surv-Adel dataset correspond to delayed mode regional dataset along the Adelie coast provided by the Survostral project and available via ftp. Adjusted values when available and only collected TSG data that exhibit quality flags=1 and 2 were used.

1.2 Auxiliary geophysical datasets

Additional EO datasets are used to characterize the geophysical conditions at the in situ measurement locations and time, and 10 days prior the measurements to get an estimate of the geophysical condition and history. As discussed in Boutin et al. (2016), the presence of vertical gradients in, and horizontal variability of, sea surface salinity indeed complicates comparison of satellite and in situ measurements. The additional EO data are used here to get a first estimates of conditions for which L-band satellite SSS measured in the first centimeters of the upper ocean within a 50-150 km diameter footprint might differ from pointwise in situ measurements performed in general between 10 and 5 m depth below the surface. The spatio-temporal variability of SSS within a satellite footprint (50–150 km) is a major issue for satellite SSS validation in the vicinity of river plumes, frontal zones, and significant precipitation. Rainfall can in some cases produce vertical salinity gradients exceeding 1 pss m^{-1}; consequently, it is recommended that satellite and in situ SSS measurements less than 3–6 h after rain events should be considered with care when used in satellite calibration/validation analyses. To identify such situation, the Pi-MEP test platform is first using CMORPH products to characterize the local value and history of rain rate and ASCAT gridded data are used to characterize the local surface wind speed and history. For validation purpose, the ISAS monthly SSS in situ analysed fields at 5 m depth are collocated and compared with the in situ SSS value. The use of ISAS is motivated by the fact that it is used in the SMOS L2 official validation protocol in which systematic comparisons of SMOS L2 retrieved SSS with ISAS are done. In complement to ISAS, monthly std climatological fields from the World Ocean Atlas (WOA13) at the in situ location and date are also used to have an a priori information of the local SSS variability.

1.2.1 CMORPH

Precipitation are estimated using the CMORPH 3-hourly products at 1/4° resolution (Joyce et al. (2004)). CMORPH (CPC MORPHing technique) produces global precipitation analyses at very high spatial and temporal resolution. This technique uses precipitation estimates that have been derived from low orbiter satellite microwave observations exclusively, and whose features are transported via spatial propagation information that is obtained entirely from geostationary satellite IR data. At present NOAA incorporate precipitation estimates derived from the passive microwaves aboard the DMSP 13, 14 and 15 (SSM/I), the NOAA-15, 16, 17 and 18 (AMSU-B), and AMSR-E and TMI aboard NASA's Aqua, TRMM and GPM spacecraft, respectively. These estimates are generated by algorithms of Ferraro (1997) for SSM/I, Ferraro et al. (2000) for AMSU-B and Kummerow et al. (2001) for TMI. Note that this technique is not a precipitation estimation algorithm but a means by which estimates from existing microwave rainfall algorithms can be combined. Therefore, this method is extremely flexible such that any precipitation estimates from any microwave satellite source can be incorporated.

With regard to spatial resolution, although the precipitation estimates are available on a grid with a spacing of 8 km (at the equator), the resolution of the individual satellite-derived estimates is coarser than that - more on the order of 12 x 15 km or so. The finer "resolution" is obtained via interpolation.

In effect, IR data are used as a means to transport the microwave-derived precipitation features during periods when microwave data are not available at a location. Propagation vector matrices are produced by computing spatial lag correlations on successive images of geostationary satellite IR which are then used to propagate the microwave derived precipitation estimates. This process governs the movement of the precipitation features only. At a given location, the shape and intensity of the precipitation features in the intervening half hour periods between microwave scans are determined by performing a time-weighting interpolation between microwave-derived features that have been propagated forward in time from the previous microwave observation and those that have been propagated backward in time from the following microwave scan. NOAA refer to this latter step as "morphing" of the features.

For the present Pi-MEP products, we only considered the 3-hourly products at 1/4 degree resolution. The entire CMORPH record (December 2002-present) for 3-hourly, 1/4 degree lat/lon resolution can be found at: `ftp://ftp.cpc.ncep.noaa.gov/precip/CMORPH_V1.0/RAW/`. CMORPH estimates cover a global belt (-180°W to 180°E) extending from 60°S to 60°N latitude and are available for the complete period of the Pi-MEP core datasets (Jan 2010-now).

1.2.2 ASCAT

Advanced SCATterometer (ASCAT) daily data produced and made available at Ifremer/CERSAT on a 0.25°x0.25° resolution grid (Bentamy and Fillon (2012)) since March 2007 are used to characterize the mean daily wind at the match-up pair location as well as the wind history during the 10-days period preceding the in situ measurement date. These wind fields are calculated based on a geostatistical method with external drift. Remotely sensed data from ASCAT are considered as observations while those from numerical model analysis (ECMWF) are associated with the external drift. The spatial and temporal structure functions for wind speed, zonal and meridional wind components are estimated from ASCAT retrievals. Furthermore, the new procedure includes a temporal interpolation of the retrievals based on the complex empirical orthogonal function (CEOF) approach, in order to enhance the sampling length of the scatterometer observations. The resulting daily wind fields involves the main known surface wind patterns as well as some variation modes associated with temporal and spatial moving features. The accuracy of the gridded winds was investigated through comparisons with moored buoy data in Bentamy

et al. (2012) and resulted in rms differences for wind speed and direction are about 1.50 m.s^{-1} and 20°.

1.2.3 ISAS

The In Situ Analysis System (ISAS), as described in Gaillard et al. (2016) is a data based re-analysis of temperature and salinity fields over the global ocean. It was initially designed to synthesize the temperature and salinity profiles collected by the ARGO program. It has been later extended to accommodate all type of vertical profile as well as time series. ISAS gridded fields are entirely based on in-situ measurements. The methodology and configuration have been conceived to preserve as much as possible the data information content and resolution. ISAS is developed and run in a research laboratory (LOPS) in close collaboration with Coriolis, one of ARGO Global Data Assembly Center and unique data provider for the Mercator operational oceanography system. At the moment the period covered starts in 2002 and only the upper 2000m are considered. The gridded fields were produced over the global ocean 70°N–70°S on a 1/2° grid by the ISAS project with datasets downloaded from the Coriolis data center (for more details on ISAS see Gaillard et al. (2009)). In the PiMEP, the product in used is the INSITU_GLO_TS_OA_NRT_OBSERVATIONS_013_002_a v6.2 NRT derived at the Coriolis data center and provided by Copernicus (www.marine.copernicus.eu/documents/PUM/CMEMS-INS-PUM-013-002-ab.pdf). The major contribution to the data set is from Argo array of profiling floats, reaching an approximate resolution of one profile every 10-days and every 3-degrees over the Satellite SSS period (http://www.umr-lops.fr/SNO-Argo/Products/ISAS-T-S-fields/); in this version SSS from thermosalinographs from ship of opportunity are not used, so that we can consider SMOS SSS validation using ship of opportunity measurements independent of ISAS. The ISAS optimal interpolation involves a structure function modeled as the sum of two Gaussian functions, each associated with specific time and space scales, resulting in a smoothing over typically 3 degrees. The smallest scale which can be retrieved with ISAS analysis is not smaller than 300–500 km (Kolodziejczyk et al. (2015)). For validation purpose, the ISAS monthly SSS fields at depth level 5 m are collocated and compared with the satellite SSS products and included in the PiMEP MDB files. In addition, the « percentage of variance » fields (PCTVAR) contained in the ISAS analyses provide information on the local variability of in situ SSS measurements within 1/2°x1/2° boxes.

1.2.4 World Ocean Atlas Climatology

The World Ocean Atlas 2013 version 2 (WOA13 V2) is a set of objectively analyzed (1° grid) climatological fields of in situ temperature, salinity and other variables provided at standard depth levels for annual, seasonal, and monthly compositing periods for the World Ocean. It also includes associated statistical fields of observed oceanographic profile data interpolated to standard depth levels on 5°, 1°, and 0.25° grids. We use these fields in complement to ISAS to characterize the climatological fields (monthly mean and std) at the match-up pairs location and date.

2 In Situ Dababase Analyses

2.1 TSG-LEGOS-DM

2.1.1 Number of SSS data as a function of time and distance to coast

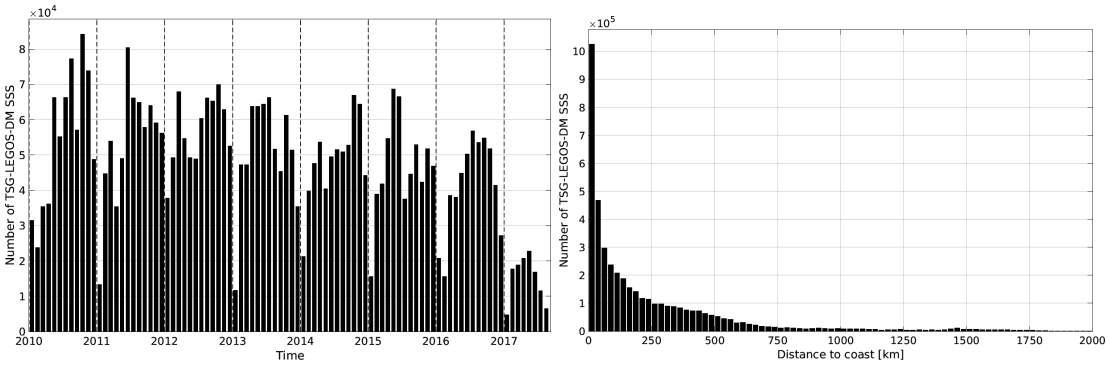

Figure 1: Number of SSS from TSG-LEGOS-DM as a function of time (left) and distance to coast (right).

2.1.2 Histogram of SSS

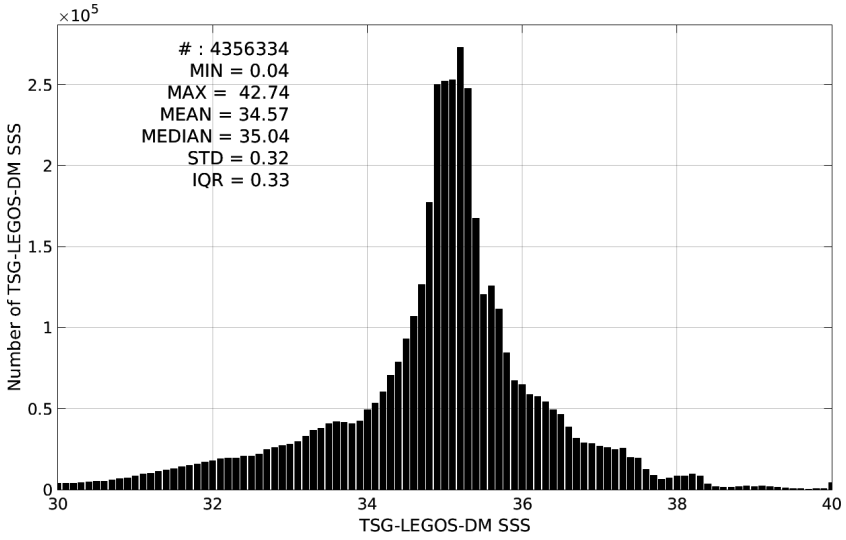

Figure 2: Distribution of SSS from TSG-LEGOS-DM per bins of 0.1.

2.1.3 Temporal mean of SSS

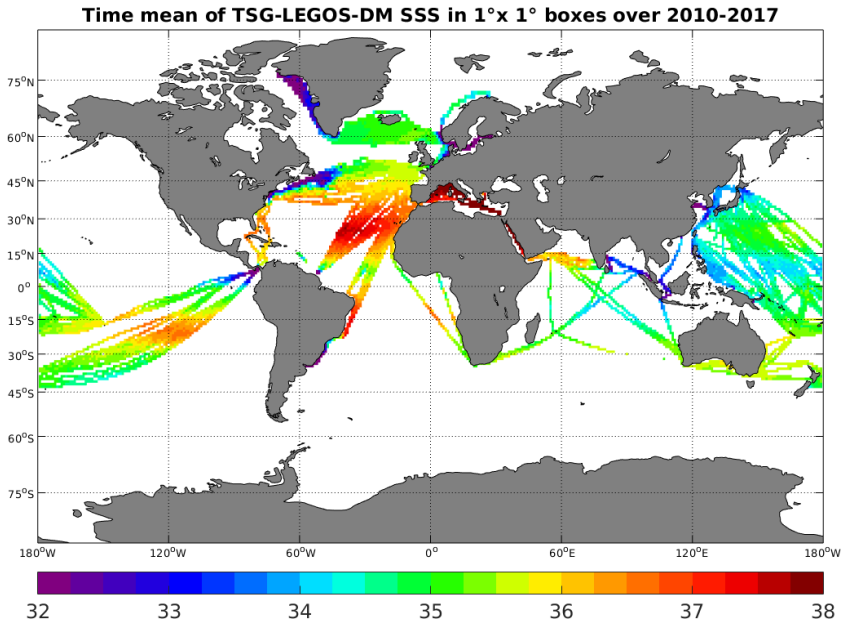

Figure 3: Time-mean SSS from TSG-LEGOS-DM in 1°x1° boxes.

2.1.4 Temporal STD of SSS

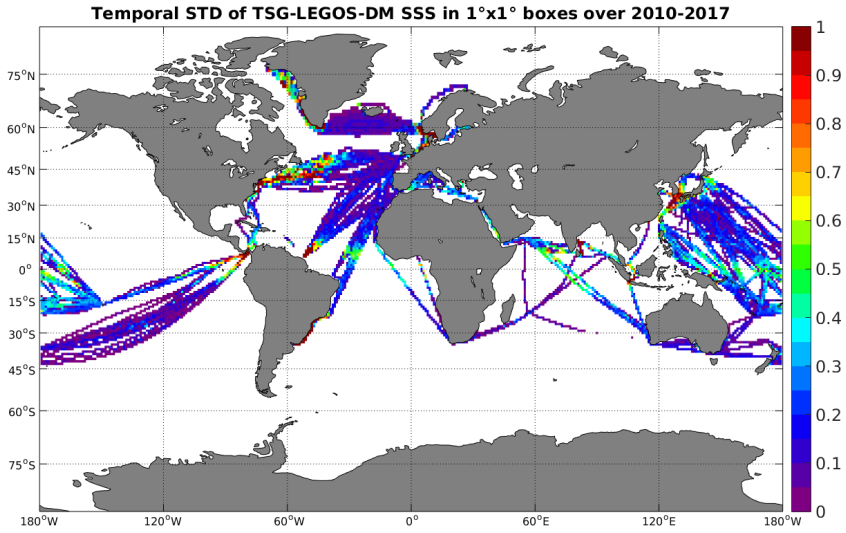

Figure 4: Temporal STD of SSS from TSG-LEGOS-DM in 1°x1° boxes.

2.1.5 Spatial density of SSS

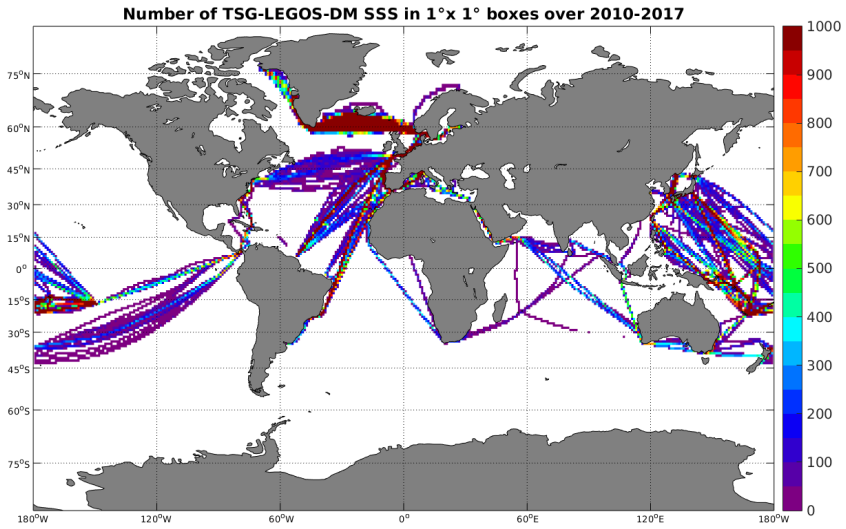

Figure 5: Number of SSS from TSG-LEGOS-DM in 1°x1° boxes.

2.1.6 ΔSSS sorted as geophysical conditions

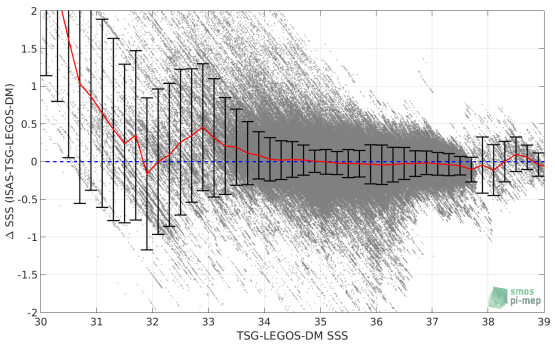

(a) TSG-LEGOS-DM SSS

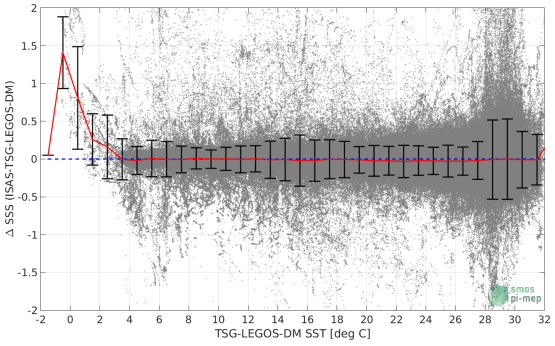

(b) TSG-LEGOS-DM SST

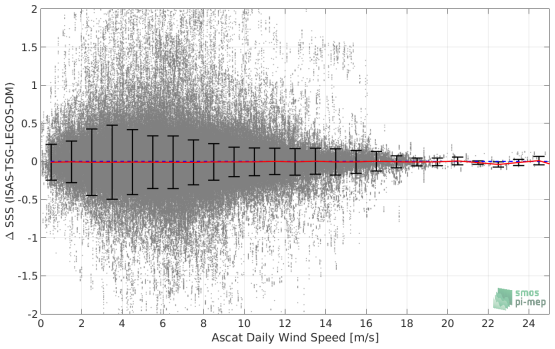

(c) ASCAT Wind Speed

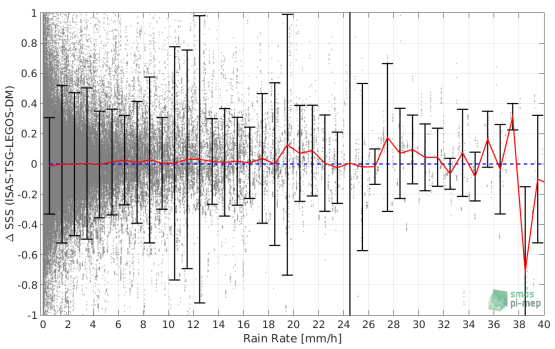

(d) CMORPH Rain rate

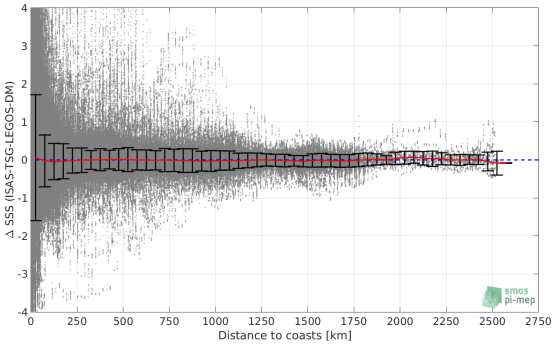

(e) Distance to coast

Figure 6: Δ SSS (ISAS - TSG-LEGOS-DM) sorted as geophysical conditions: TSG-LEGOS-DM SSS a), TSG-LEGOS-DM SST b), ASCAT Wind speed c), CMORPH rain rate d) and distance to coast (e).

2.1.7 Conditional analyses

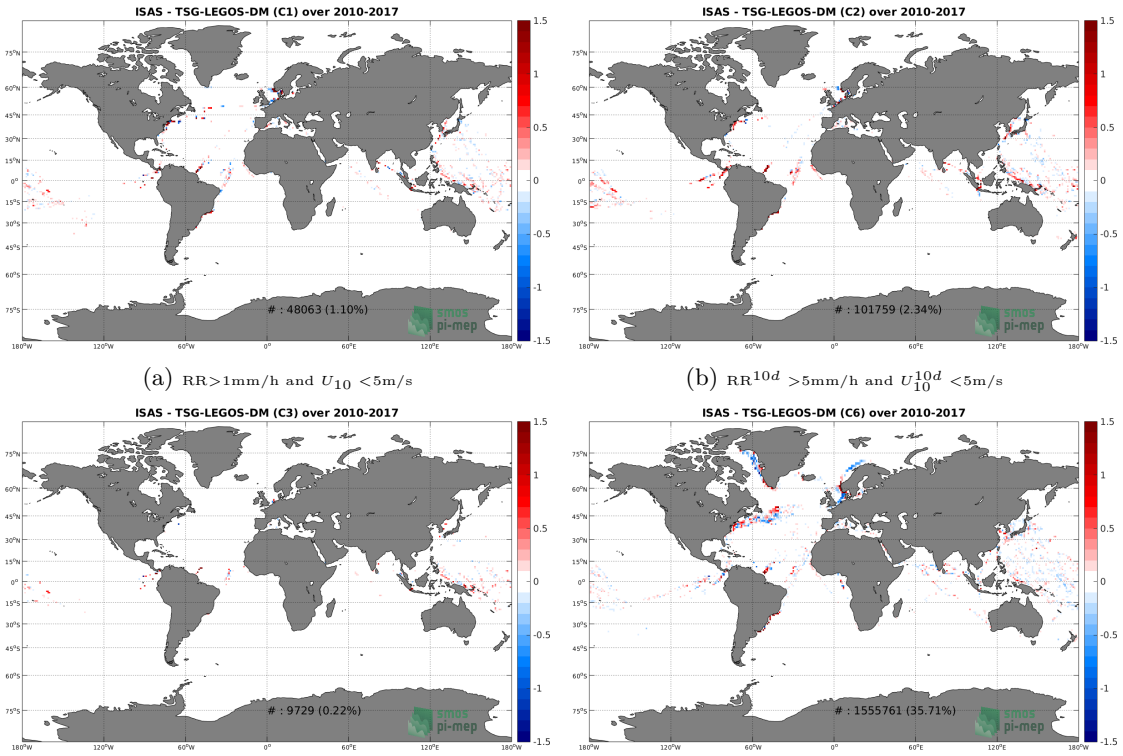

(a) RR>1mm/h and U_{10} <5m/s

(b) RR^{10d} >5mm/h and U_{10}^{10d} <5m/s

(c) C1 U C2

(d) Locations where WOA2013 SSS STD>0.2

Figure 7: Temporal mean of ΔSSS (ISAS - TSG-LEGOS-DM) for 4 different subdatasets corresponding to C1 (a), C2 (b), C3 (c) and C6 (f).

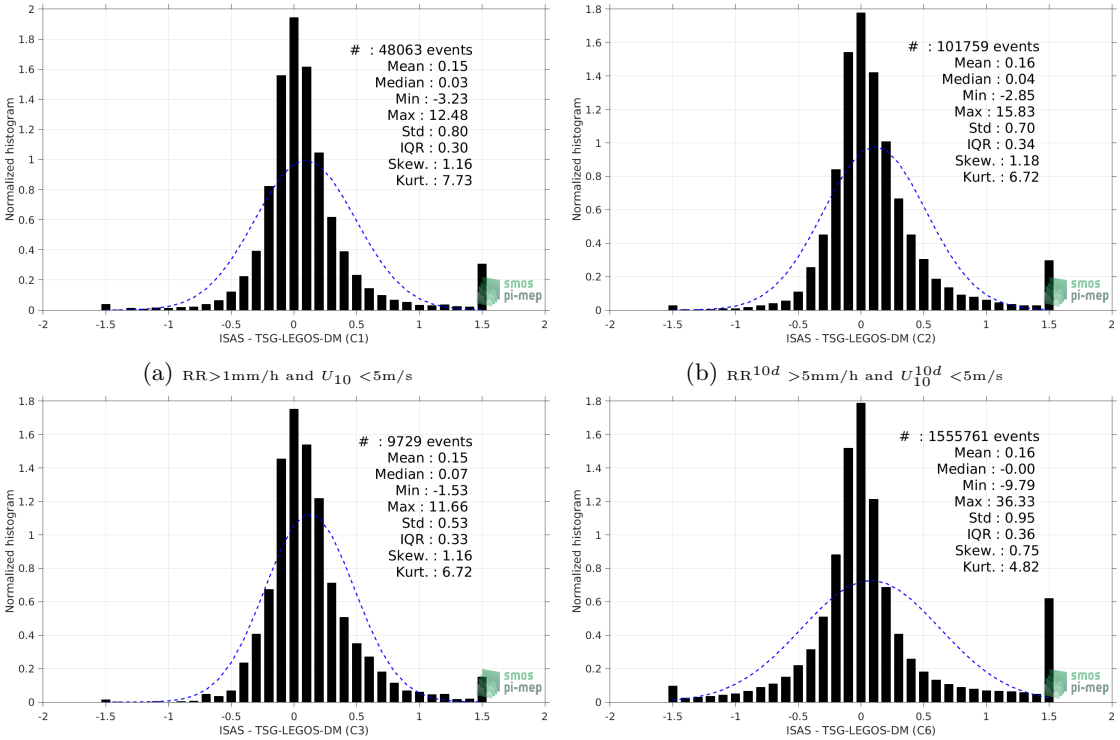

(a) RR>1mm/h and U_{10} <5m/s

(b) RR^{10d} >5mm/h and U_{10}^{10d} <5m/s

(c) C1 U C2

(d) Locations where WOA2013 SSS STD>0.2

Figure 8: Normalized histogram of ΔSSS (ISAS - TSG-LEGOS-DM) for 4 different subdatasets corresponding to C1 (a), C2 (b), C3 (c) and C6 (f).

2.2 TSG-GOSUD-Research-vessel

2.2.1 Number of SSS data as a function of time and distance to coast

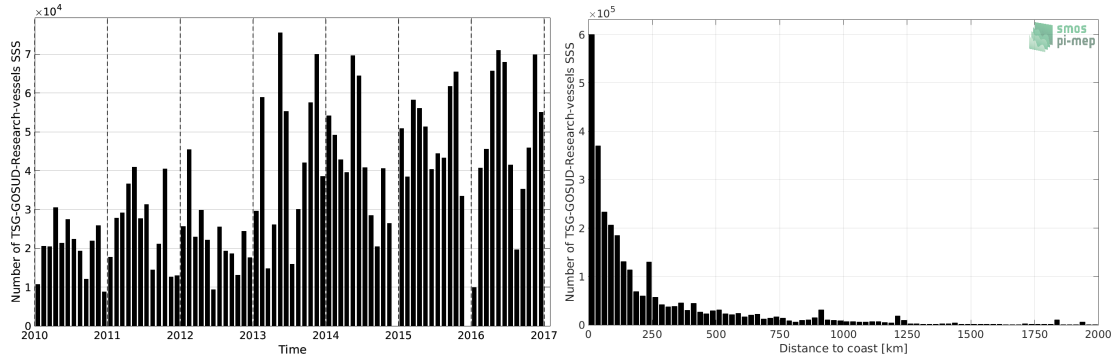

Figure 9: Number of SSS from TSG-GOSUD-Research-vessel as a function of time (left) and distance to coast (right).

2.2.2 Histogram of SSS

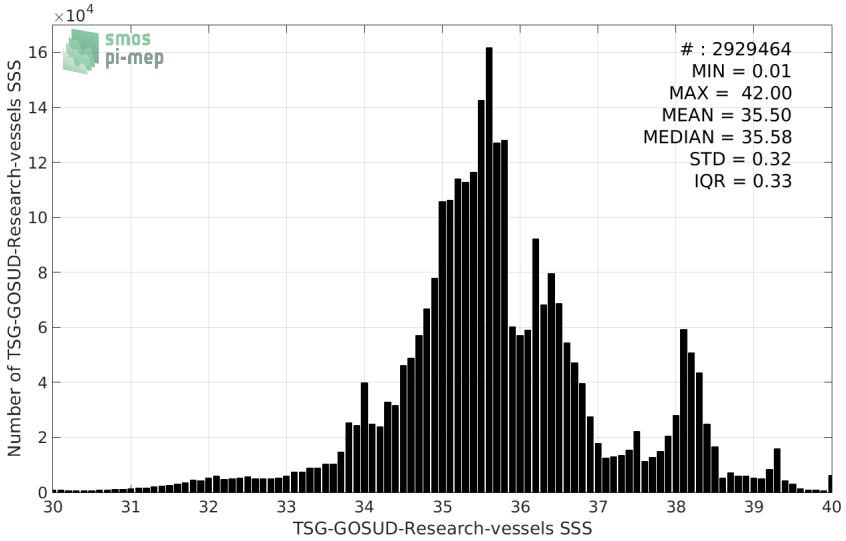

Figure 10: Distribution of SSS from TSG-GOSUD-Research-vessel per bins of 0.1.

2.2.3 Temporal mean of SSS

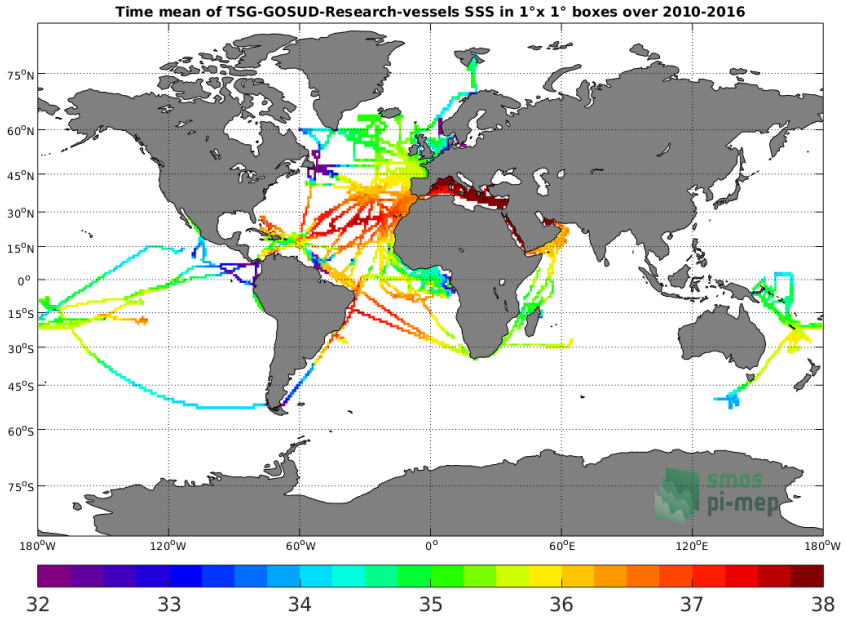

Figure 11: Time-mean SSS from TSG-GOSUD-Research-vessel in 1°x1° boxes.

2.2.4 Temporal STD of SSS

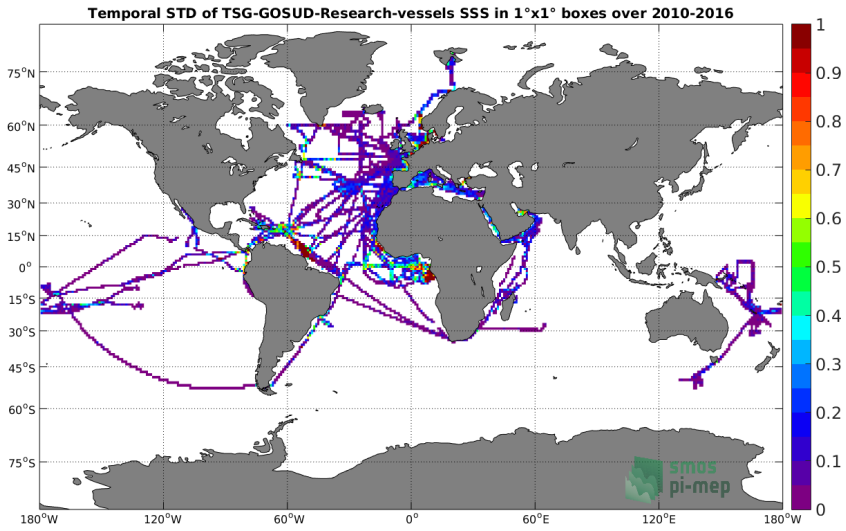

Figure 12: Temporal STD of SSS from TSG-GOSUD-Research-vessel in 1°x1° boxes.

2.2.5 Spatial density of SSS

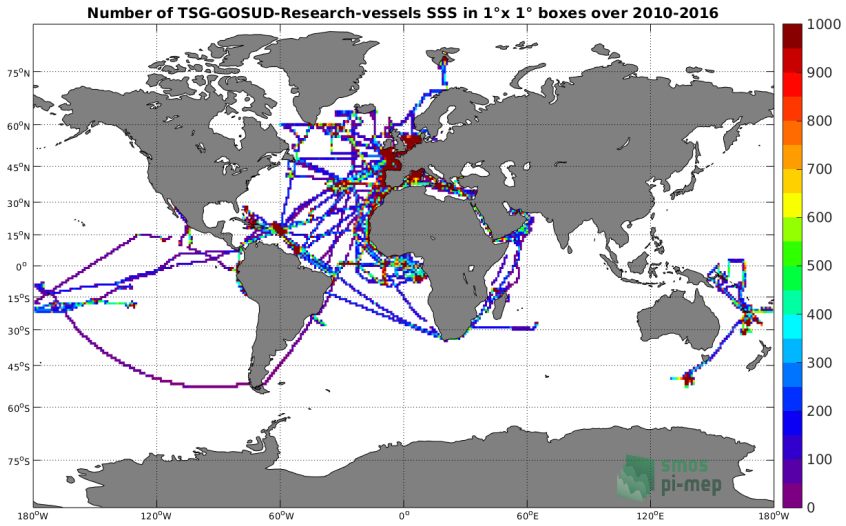

Figure 13: Number of SSS from TSG-GOSUD-Research-vessel in 1°x1° boxes.

2.2.6 ΔSSS sorted as geophysical conditions

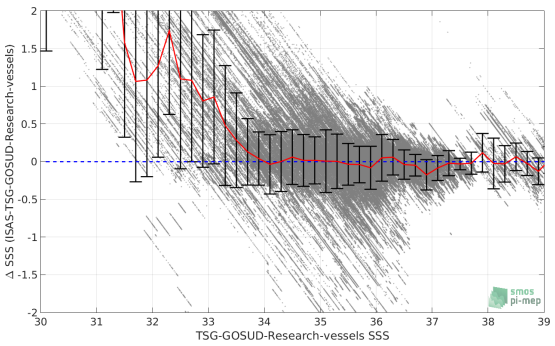

(a) TSG-GOSUD-Research-vessel SSS

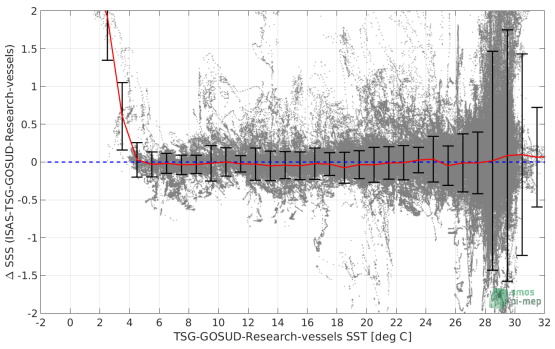

(b) TSG-GOSUD-Research-vessel SST

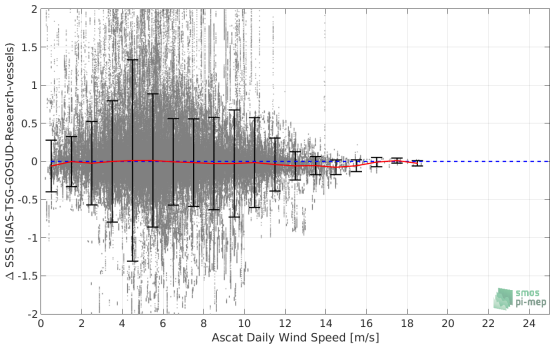

(c) ASCAT Wind Speed

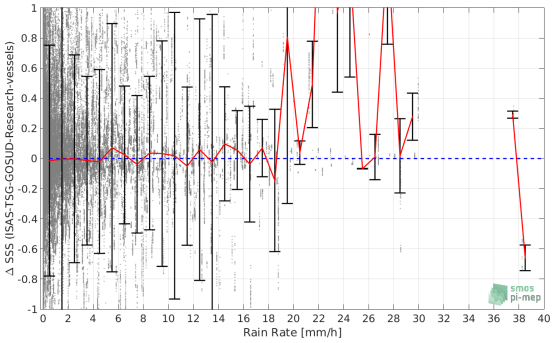

(d) CMORPH Rain rate

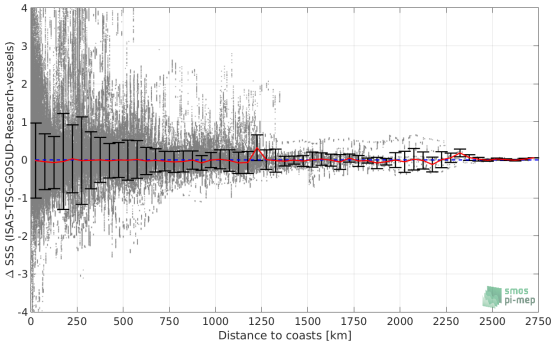

(e) Distance to coast

Figure 14: Δ SSS (ISAS - TSG-GOSUD-Research-vessel) sorted as geophysical conditions: TSG-GOSUD-Research-vessel SSS a), TSG-GOSUD-Research-vessel SST b), ASCAT Wind speed c), CMORPH rain rate d) and distance to coast (e).

2.2.7 Conditional analyses

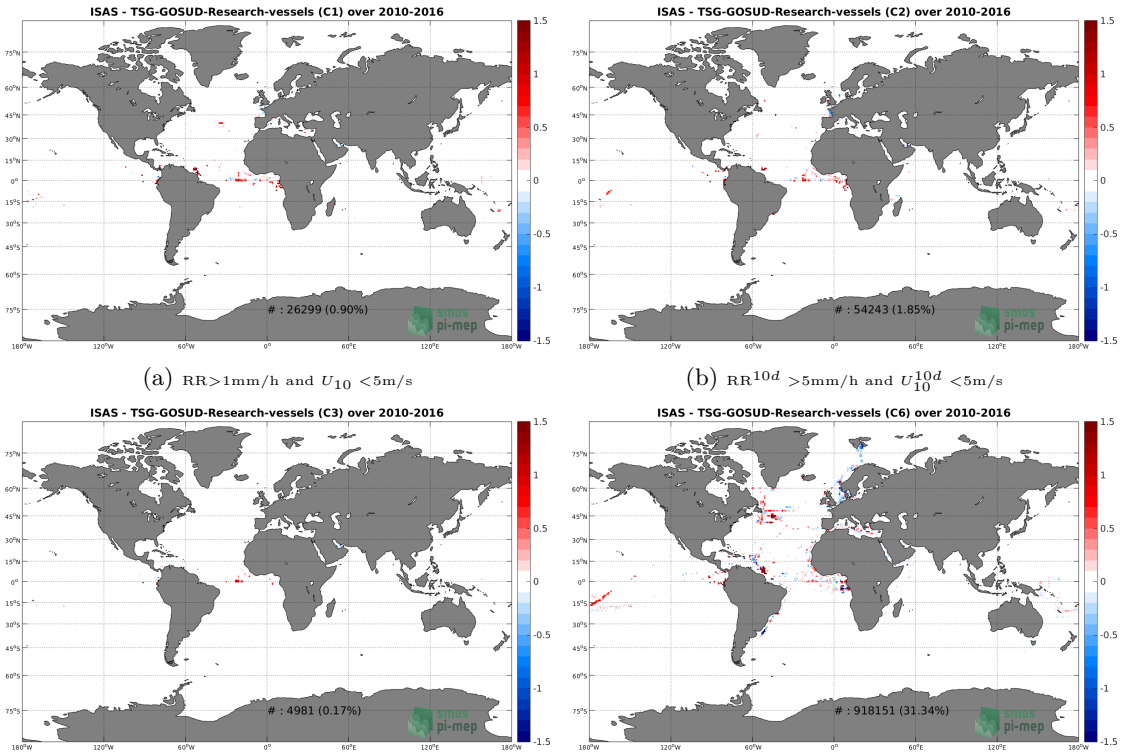

(a) RR>1mm/h and U_{10} <5m/s

(b) RR^{10d} >5mm/h and U_{10}^{10d} <5m/s

(c) C1 U C2

(d) Locations where WOA2013 SSS STD>0.2

Figure 15: Temporal mean of ΔSSS (ISAS - TSG-GOSUD-Research-vessel) for 4 different sub-datasets corresponding to C1 (a), C2 (b), C3 (c) and C6 (f).

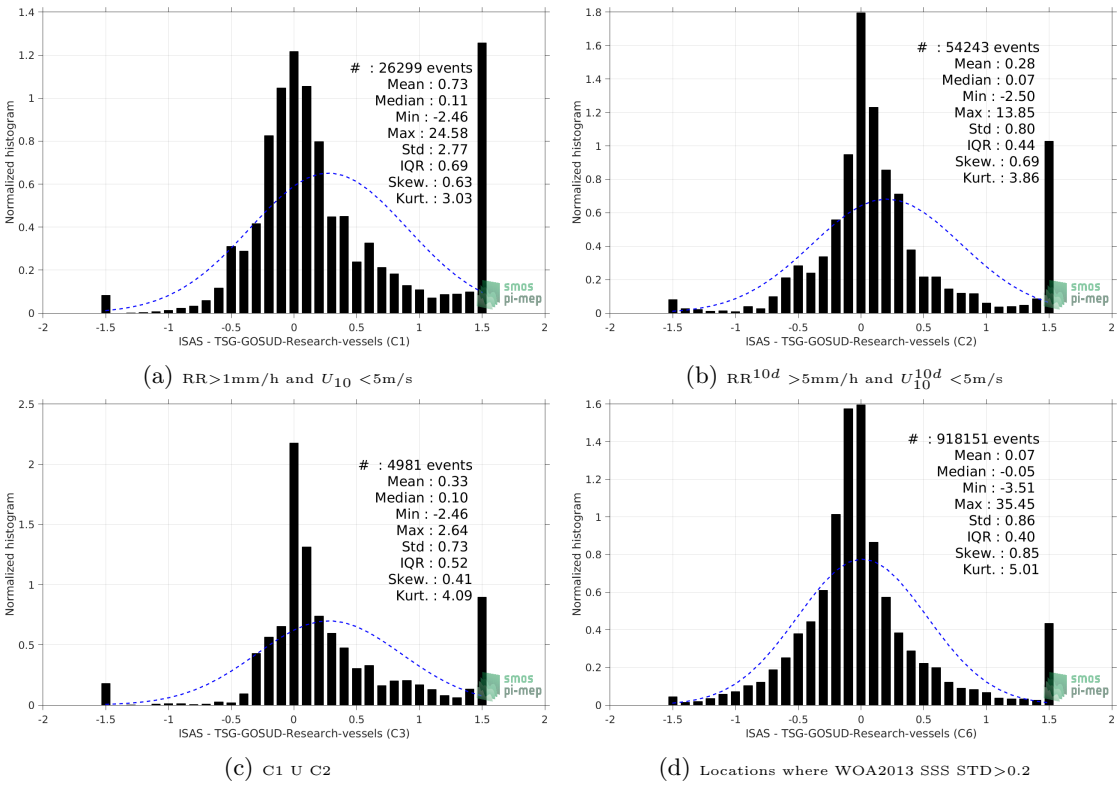

(a) RR>1mm/h and U_{10} <5m/s

(b) RR^{10d} >5mm/h and U_{10}^{10d} <5m/s

(c) C1 U C2

(d) Locations where WOA2013 SSS STD>0.2

Figure 16: Normalized histogram of ΔSSS (ISAS - TSG-GOSUD-Research-vessel) for 4 different subdatasets corresponding to C1 (a), C2 (b), C3 (c) and C6 (f).

2.3 TSG-GOSUD-Sailing-ship

2.3.1 Number of SSS data as a function of time and distance to coast

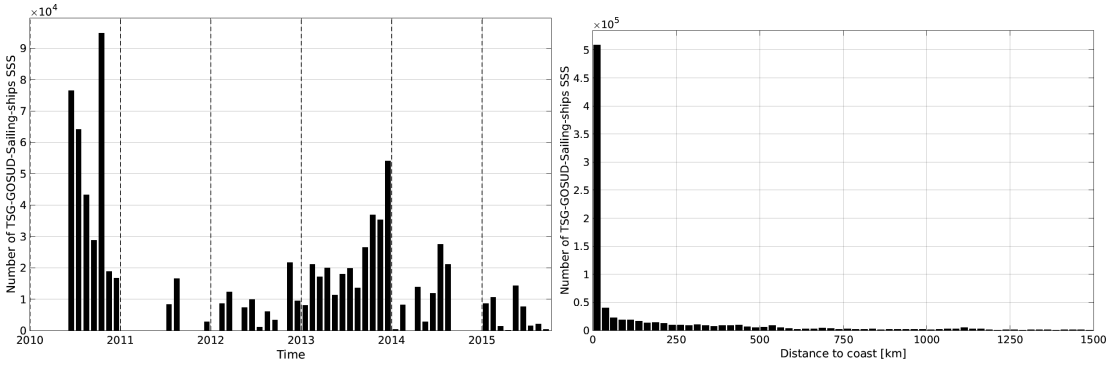

Figure 17: Number of SSS from TSG-GOSUD-Sailing-ship as a function of time (left) and distance to coast (right).

2.3.2 Histogram of SSS

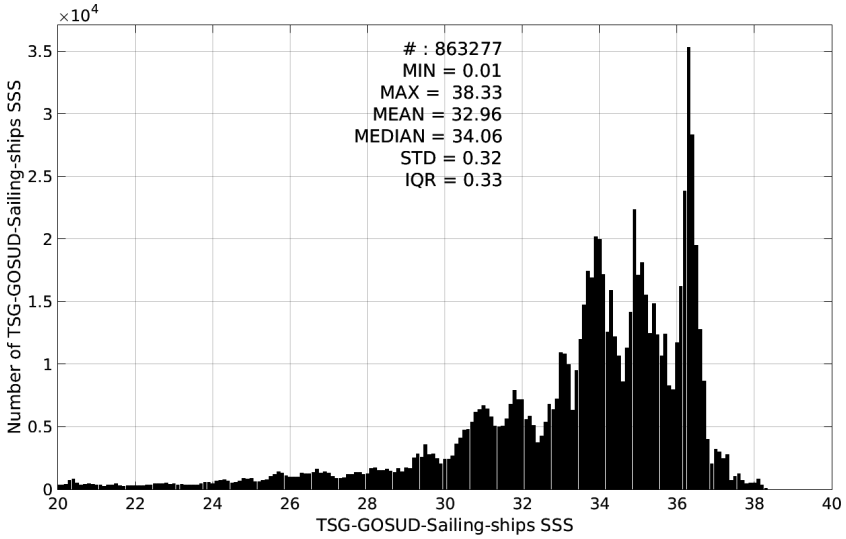

Figure 18: Distribution of SSS from TSG-GOSUD-Sailing-ship per bins of 0.1.

2.3.3 Temporal mean of SSS

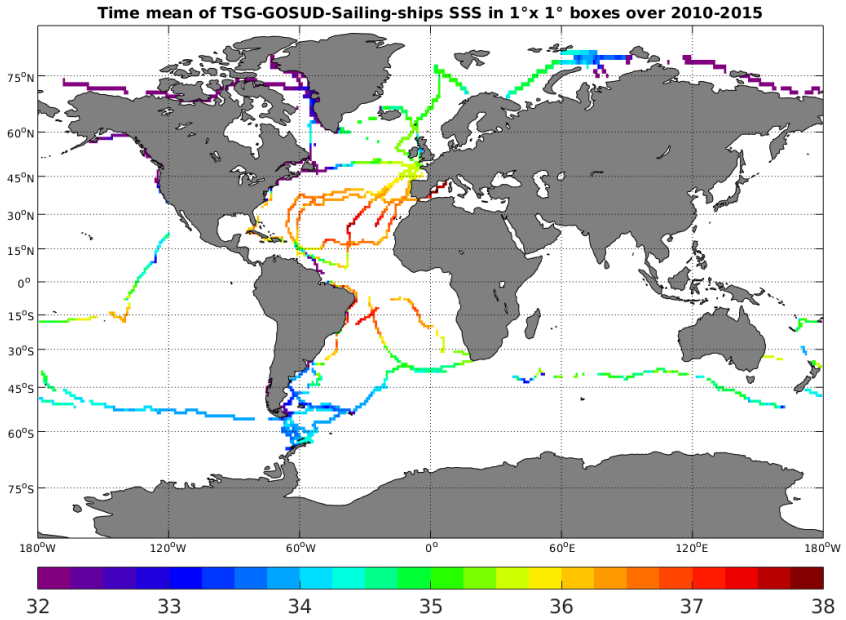

Figure 19: Time-mean SSS from TSG-GOSUD-Sailing-ship in 1°x1° boxes.

2.3.4 Temporal STD of SSS

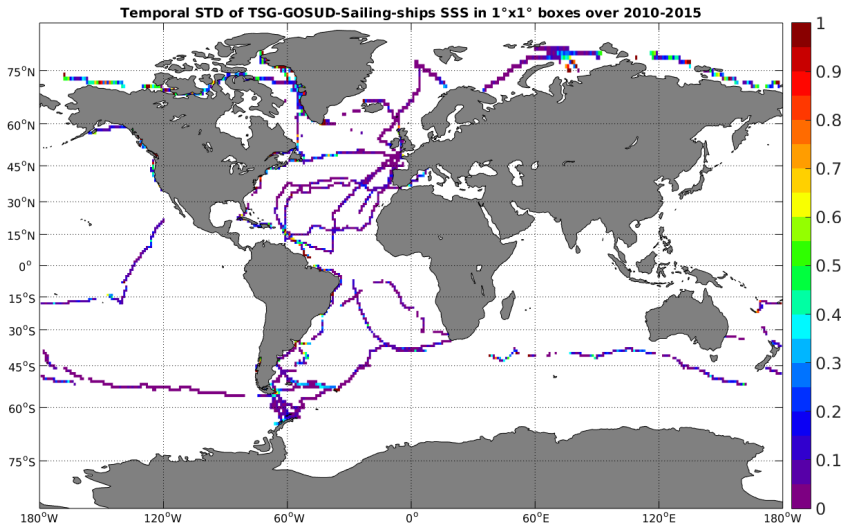

Figure 20: Temporal STD of SSS from TSG-GOSUD-Sailing-ship in 1°x1° boxes.

2.3.5 Spatial density of SSS

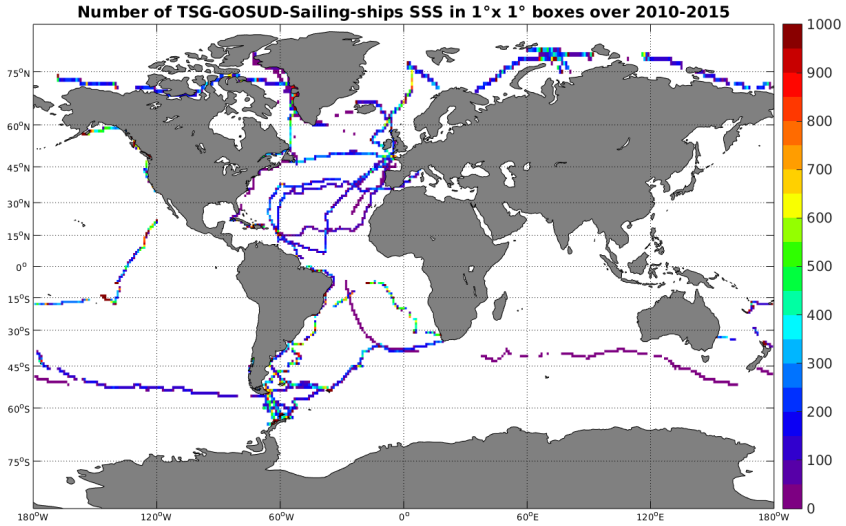

Figure 21: Number of SSS from TSG-GOSUD-Sailing-ship in 1°x1° boxes.

2.3.6 ΔSSS sorted as geophysical conditions

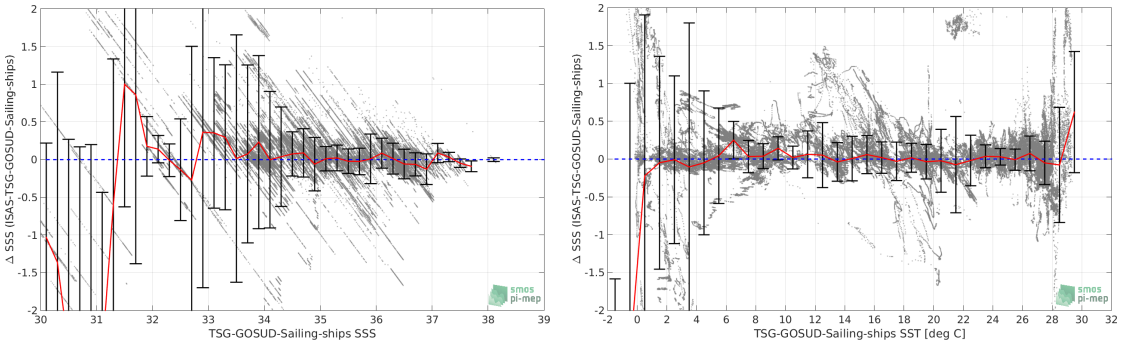

(a) TSG-GOSUD-Sailing-ship SSS

(b) TSG-GOSUD-Sailing-ship SST

(c) ASCAT Wind Speed

(d) CMORPH Rain rate

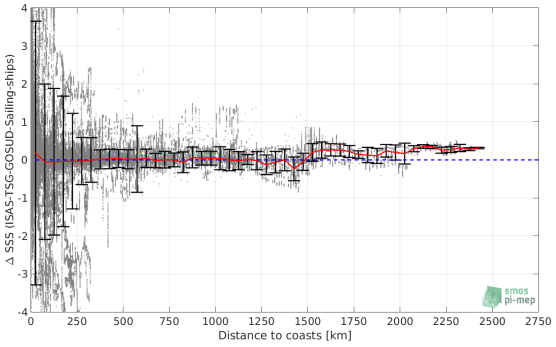

(e) Distance to coast

Figure 22: Δ SSS (ISAS - TSG-GOSUD-Sailing-ship) sorted as geophysical conditions: TSG-GOSUD-Sailing-ship SSS a), TSG-GOSUD-Sailing-ship SST b), ASCAT Wind speed c), CMORPH rain rate d) and distance to coast (e).

2.3.7 Conditional analyses

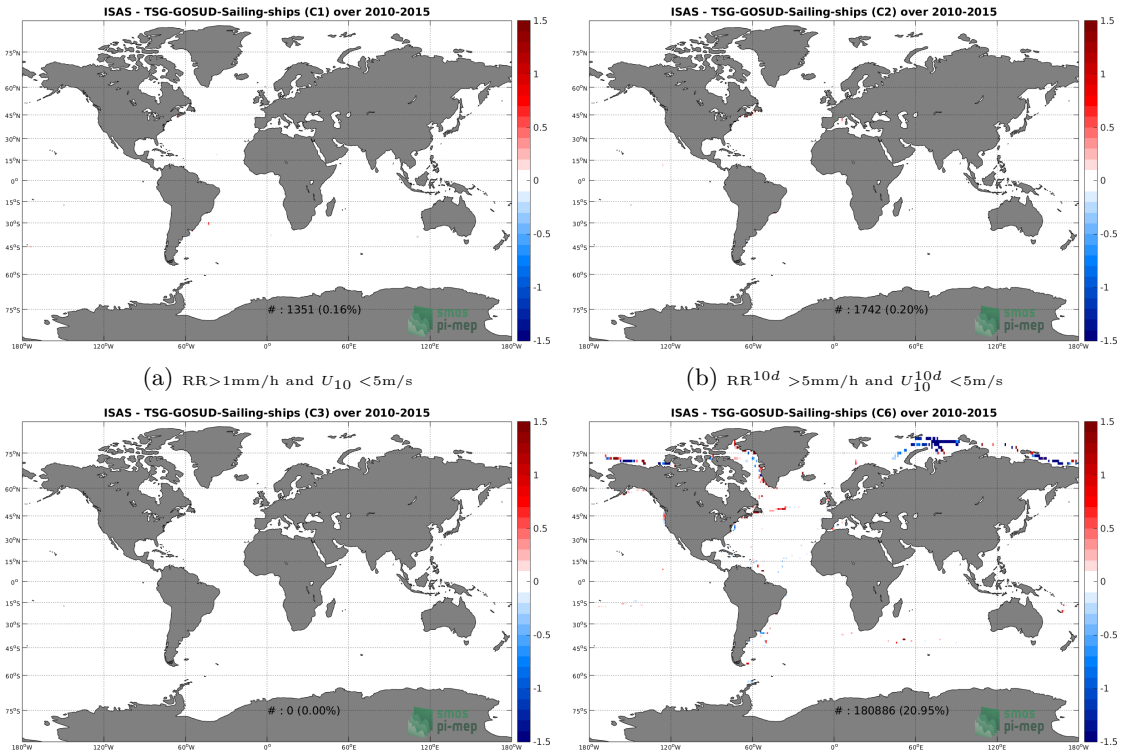

(a) RR>1mm/h and U_{10} <5m/s

(b) RR^{10d} >5mm/h and U_{10}^{10d} <5m/s

(c) C1 U C2

(d) Locations where WOA2013 SSS STD>0.2

Figure 23: Temporal mean of ΔSSS (ISAS - TSG-GOSUD-Sailing-ship) for 4 different sub-datasets corresponding to C1 (a), C2 (b), C3 (c) and C6 (f).

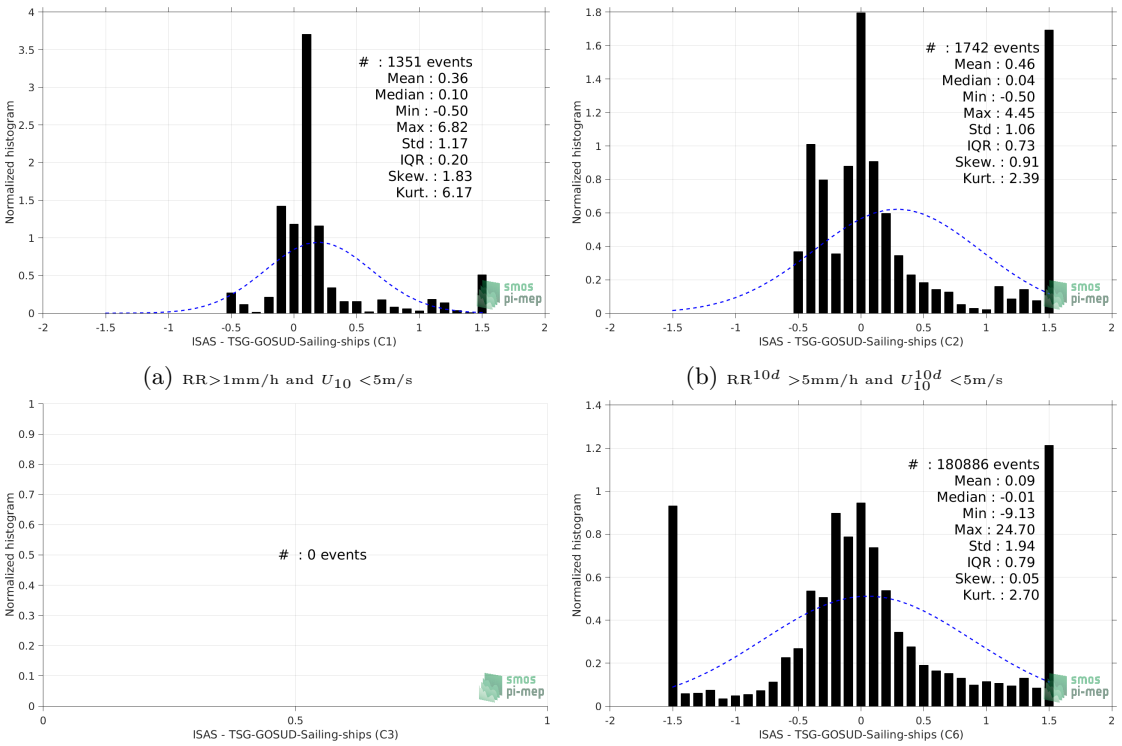

(a) RR>1mm/h and U_{10} <5m/s

(b) RR^{10d} >5mm/h and U_{10}^{10d} <5m/s

(c) C1 U C2

(d) Locations where WOA2013 SSS STD>0.2

Figure 24: Normalized histogram of ΔSSS (ISAS - TSG-GOSUD-Sailing-ship) for 4 different subdatasets corresponding to C1 (a), C2 (b), C3 (c) and C6 (f).

2.4 TSG-SAMOS

2.4.1 Number of SSS data as a function of time and distance to coast

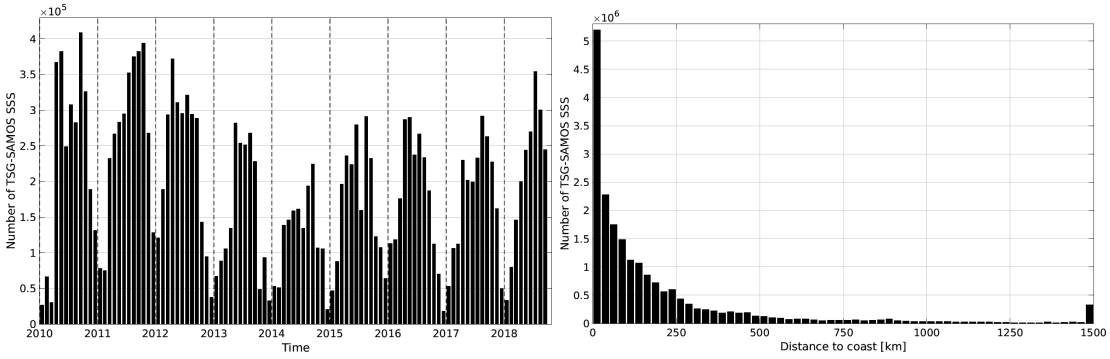

Figure 25: Number of SSS from TSG-SAMOS as a function of time (left) and distance to coast (right).

2.4.2 Histogram of SSS

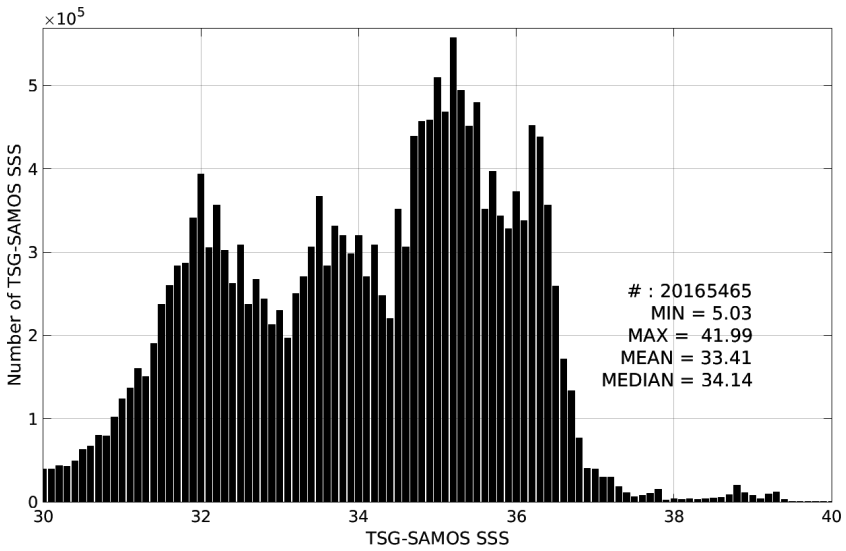

Figure 26: Distribution of SSS from TSG-SAMOS per bins of 0.1.

2.4.3 Temporal mean of SSS

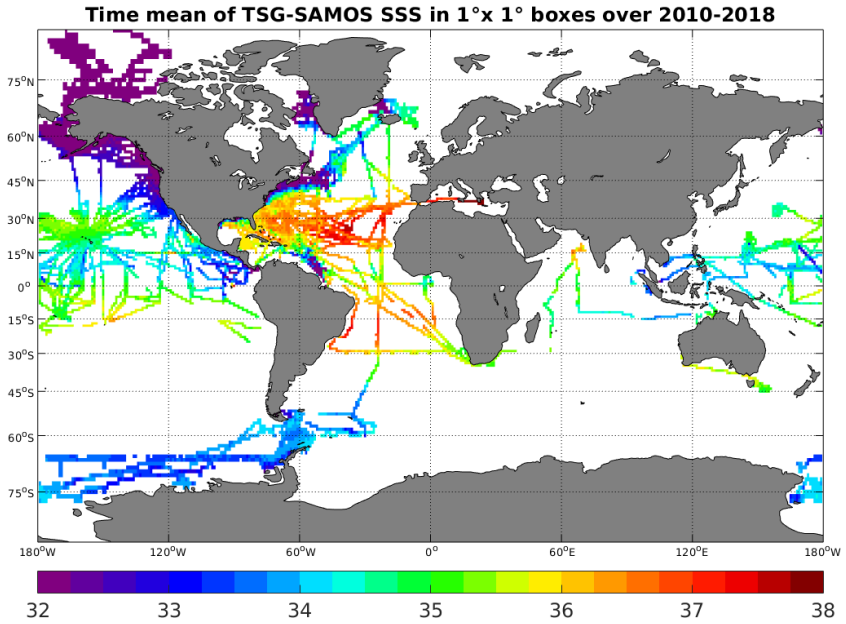

Figure 27: Time-mean SSS from TSG-SAMOS in 1°x1° boxes.

2.4.4 Temporal STD of SSS

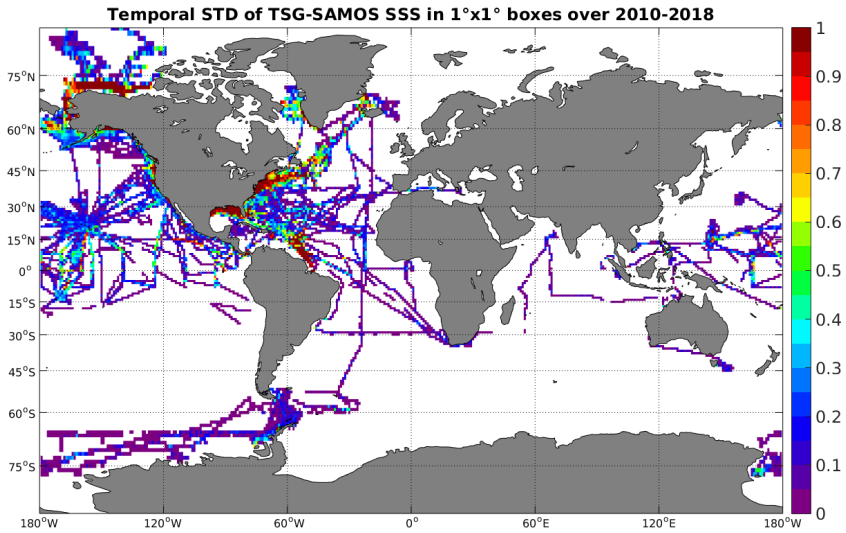

Figure 28: Temporal STD of SSS from TSG-SAMOS in 1°x1° boxes.

2.4.5 Spatial density of SSS

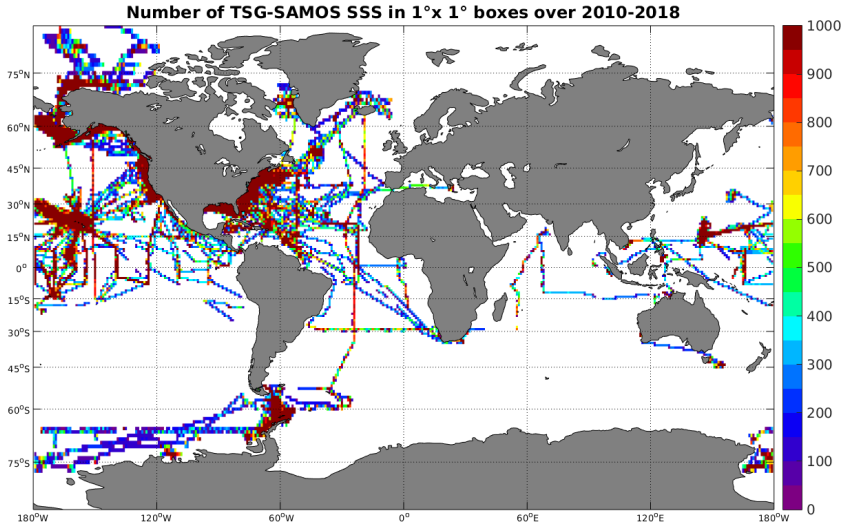

Figure 29: Number of SSS from TSG-SAMOS in 1°x1° boxes.

2.4.6 ΔSSS sorted as geophysical conditions

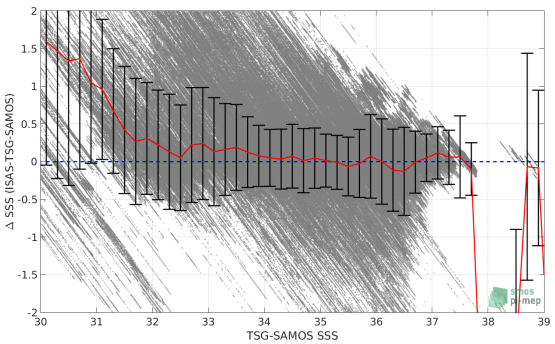

(a) TSG-SAMOS SSS

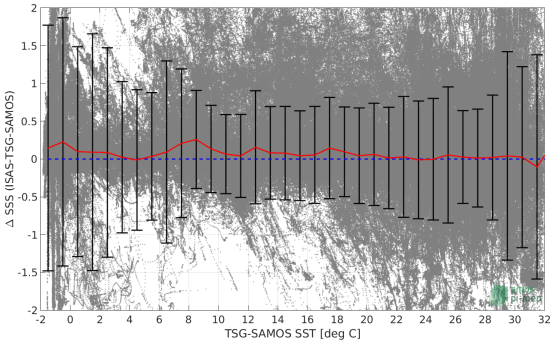

(b) TSG-SAMOS SST

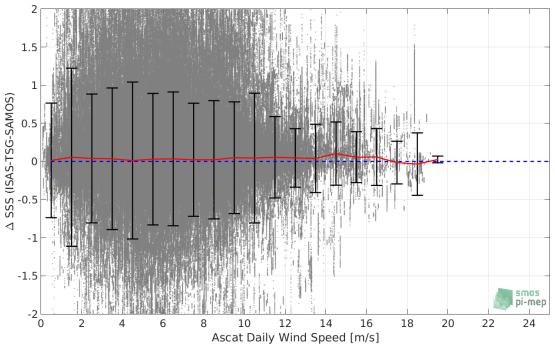

(c) ASCAT Wind Speed

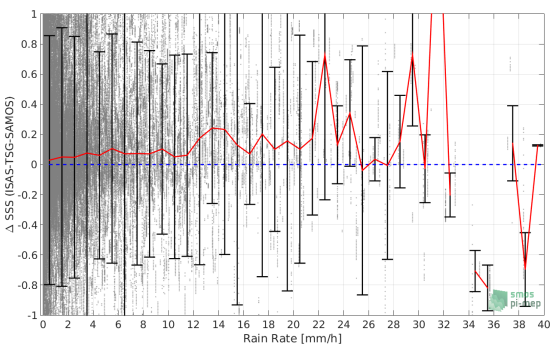

(d) CMORPH Rain rate

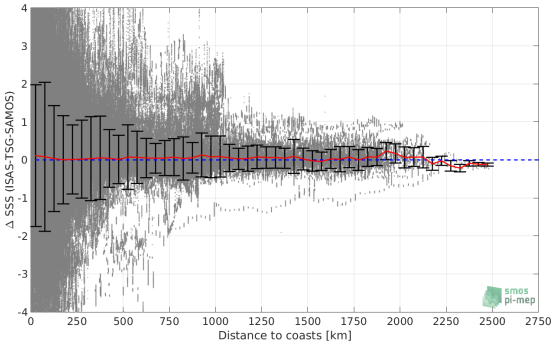

(e) Distance to coast

Figure 30: Δ SSS (ISAS - TSG-SAMOS) sorted as geophysical conditions: TSG-SAMOS SSS a), TSG-SAMOS SST b), ASCAT Wind speed c), CMORPH rain rate d) and distance to coast (e).

2.4.7 Conditional analyses

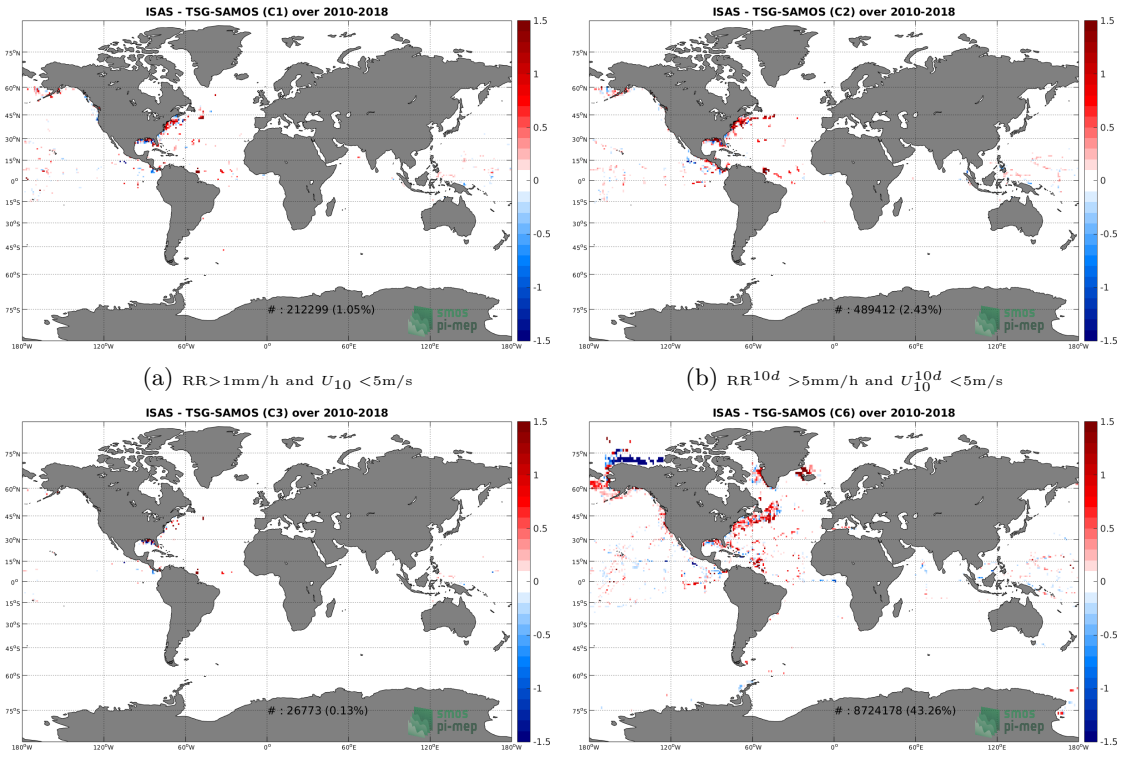

(a) RR>1mm/h and U_{10} <5m/s

(b) RR^{10d} >5mm/h and U_{10}^{10d} <5m/s

(c) C1 U C2

(d) Locations where WOA2013 SSS STD>0.2

Figure 31: Temporal mean of ΔSSS (ISAS - TSG-SAMOS) for 4 different subdatasets corresponding to C1 (a), C2 (b), C3 (c) and C6 (f).

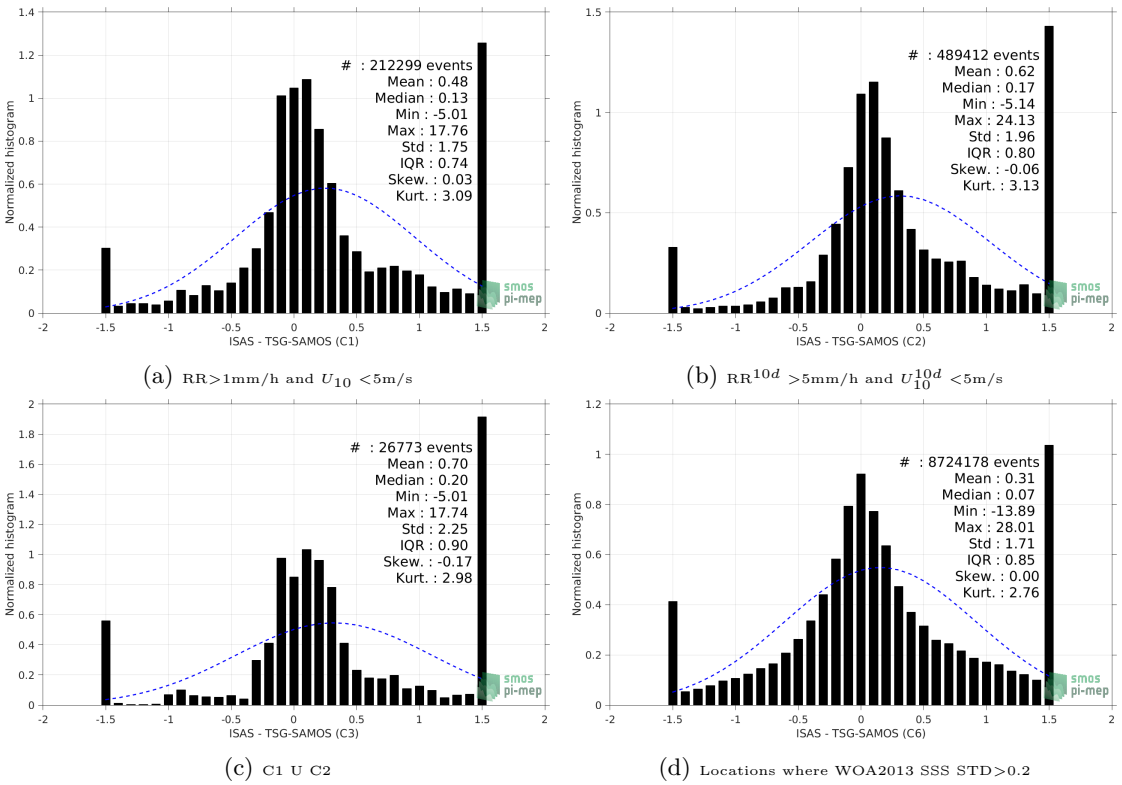

(a) RR>1mm/h and U_{10} <5m/s

(b) RR^{10d} >5mm/h and U_{10}^{10d} <5m/s

(c) C1 U C2

(d) Locations where WOA2013 SSS STD>0.2

Figure 32: Normalized histogram of ΔSSS (ISAS - TSG-SAMOS) for 4 different subdatasets corresponding to C1 (a), C2 (b), C3 (c) and C6 (f).

2.5 TSG-LEGOS-Survostral

2.5.1 Number of SSS data as a function of time and distance to coast

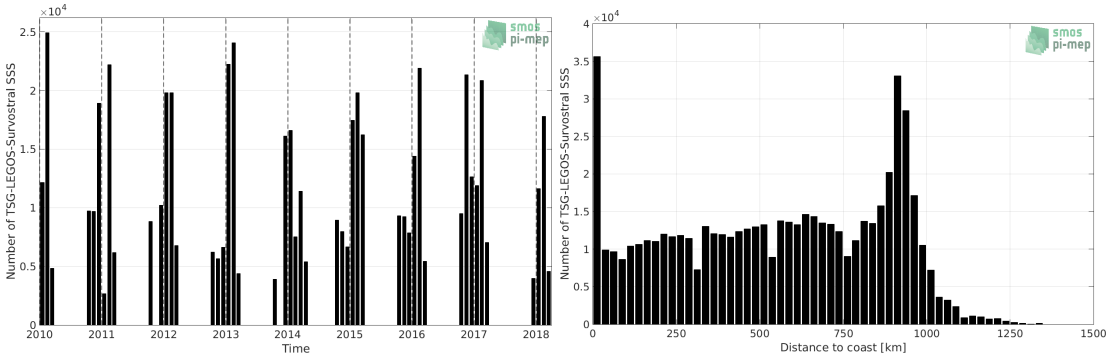

Figure 33: Number of SSS from TSG-LEGOS-Survostral as a function of time (left) and distance to coast (right).

2.5.2 Histogram of SSS

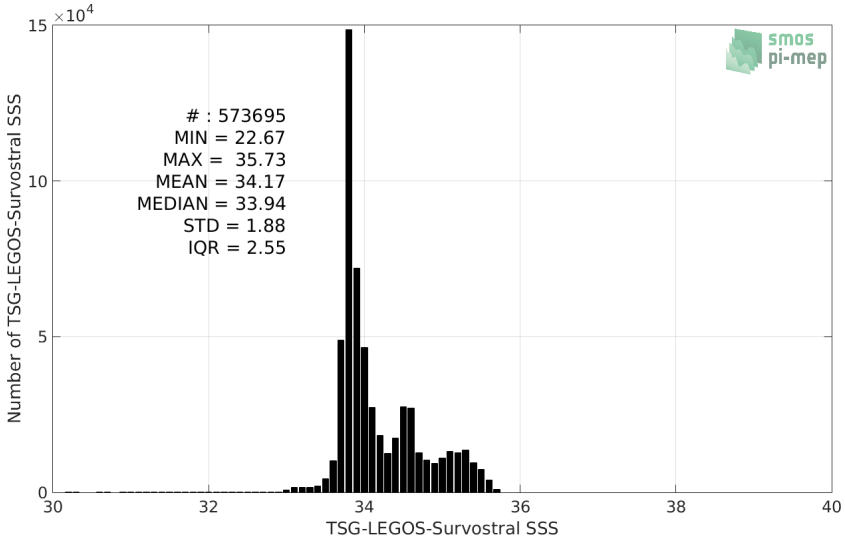

Figure 34: Distribution of SSS from TSG-LEGOS-Survostral per bins of 0.1.

2.5.3 Temporal mean of SSS

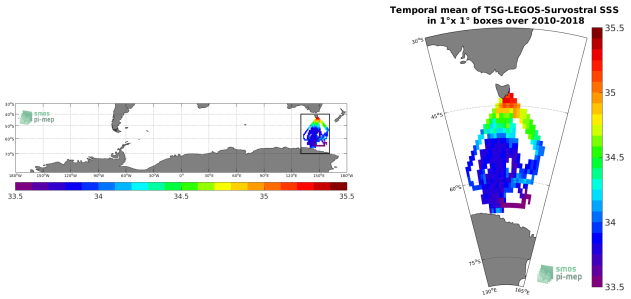

Figure 35: Time-mean SSS from TSG-LEGOS-Survostral in 1°x1° boxes.

2.5.4 Temporal STD of SSS

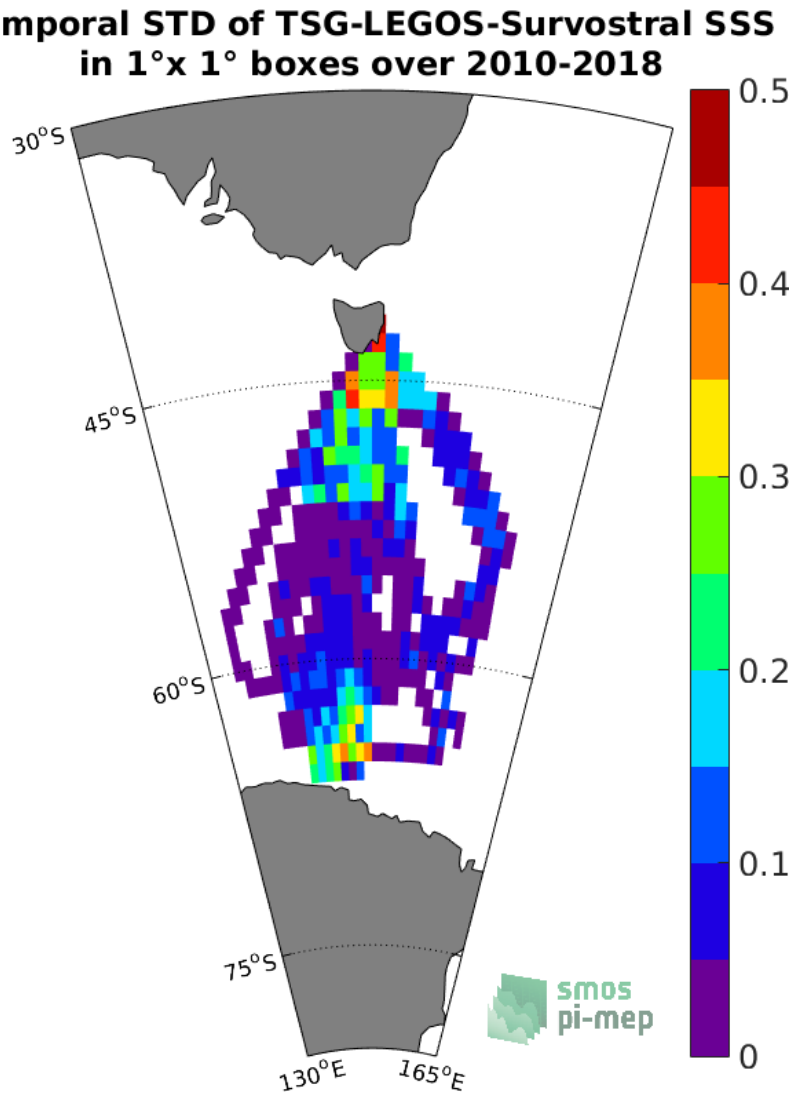

Figure 36: Temporal STD of SSS from TSG-LEGOS-Survostral in 1°x1° boxes.

2.5.5 Spatial density of SSS

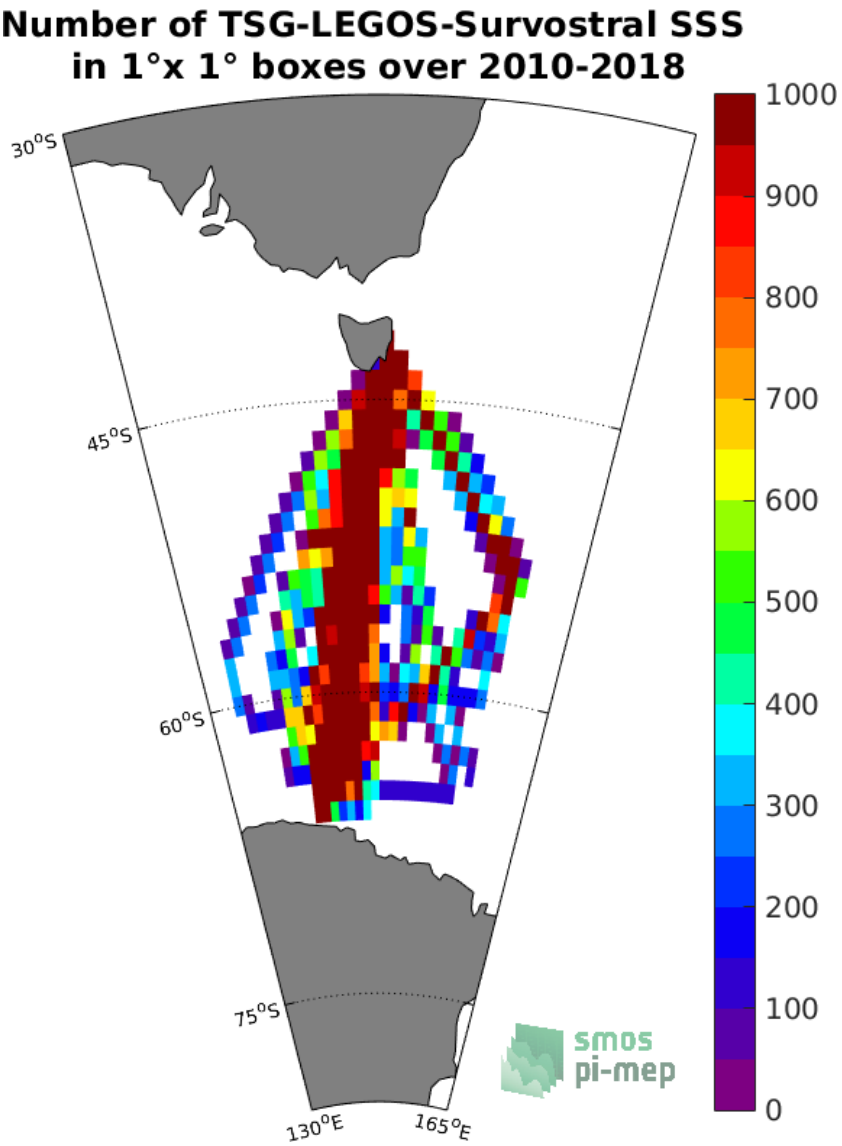

Figure 37: Number of SSS from TSG-LEGOS-Survostral in 1°x1° boxes.

2.5.6 ΔSSS sorted as geophysical conditions

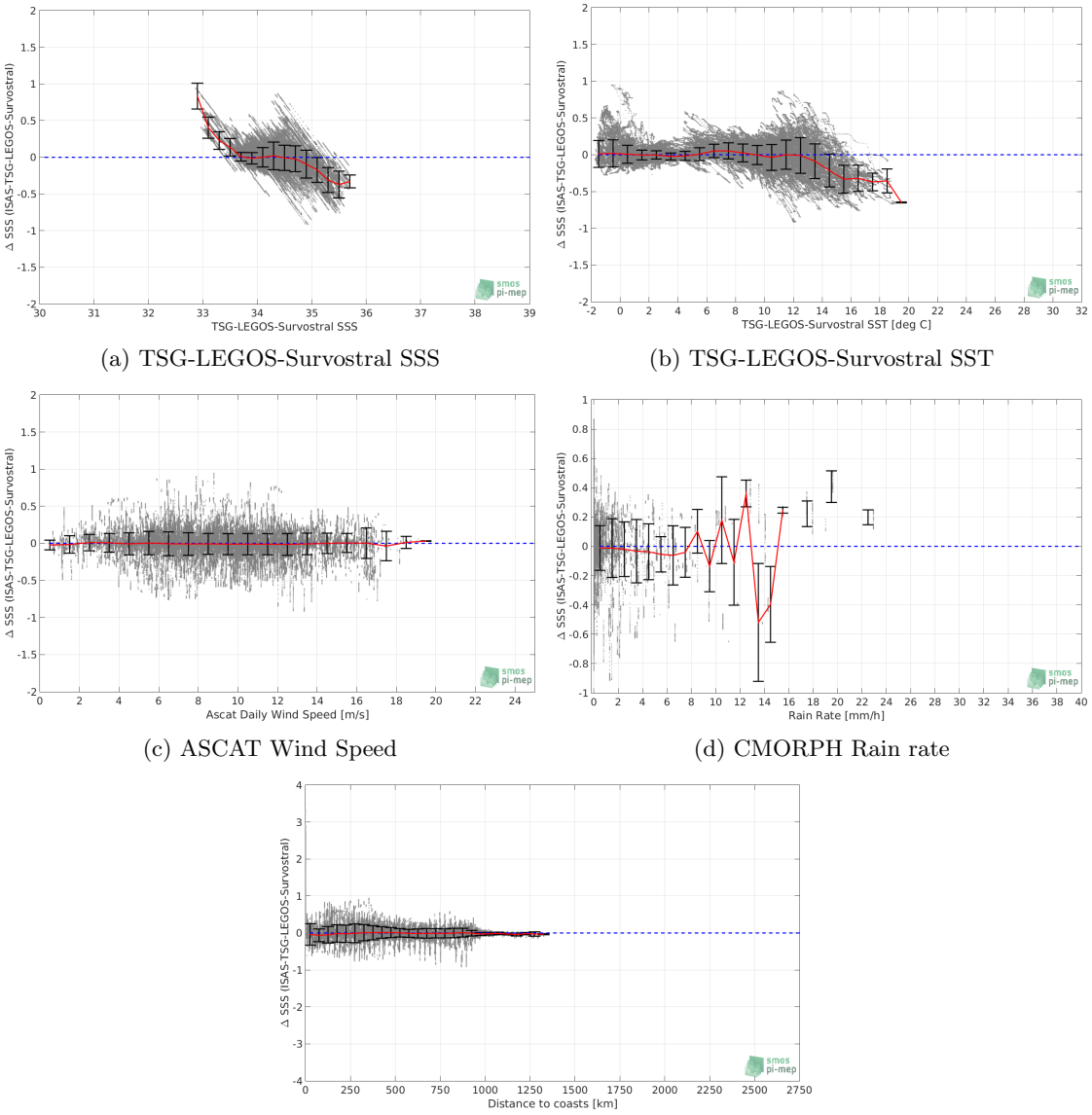

(a) TSG-LEGOS-Survostral SSS

(b) TSG-LEGOS-Survostral SST

(c) ASCAT Wind Speed

(d) CMORPH Rain rate

(e) Distance to coast

Figure 38: Δ SSS (ISAS - TSG-LEGOS-Survostral) sorted as geophysical conditions: TSG-LEGOS-Survostral SSS a), TSG-LEGOS-Survostral SST b), ASCAT Wind speed c), CMORPH rain rate d) and distance to coast (e).

2.5.7 Conditional analyses

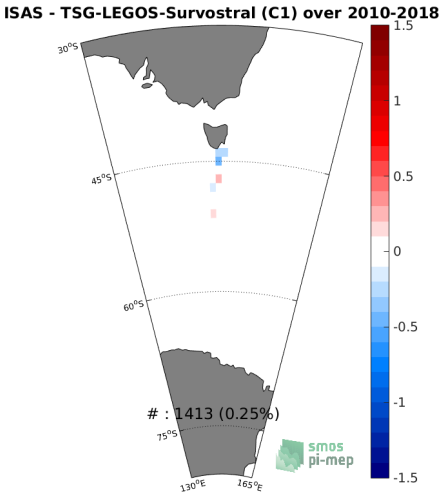

(a) RR>1mm/h and U_{10} <5m/s

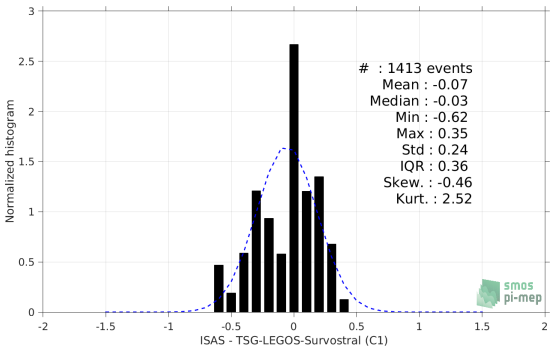

(b) RR>1mm/h and U_{10} <5m/s

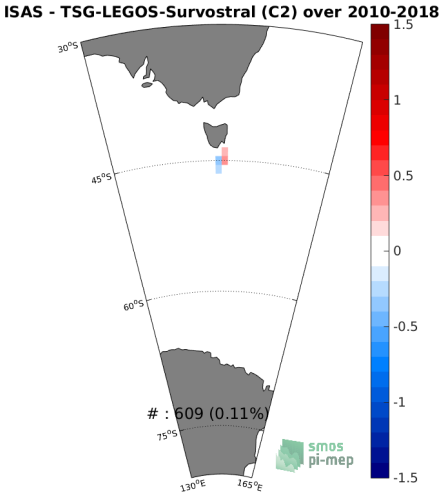

(c) RR^{10d} >5mm/h and U_{10}^{10d} <5m/s

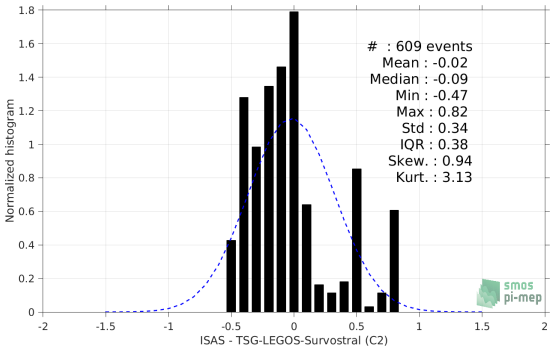

(d) RR^{10d} >5mm/h and U_{10}^{10d} <5m/s

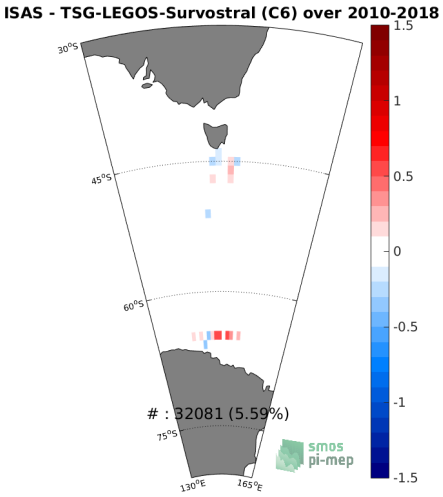

(e) Locations where WOA2013 SSS STD>0.2

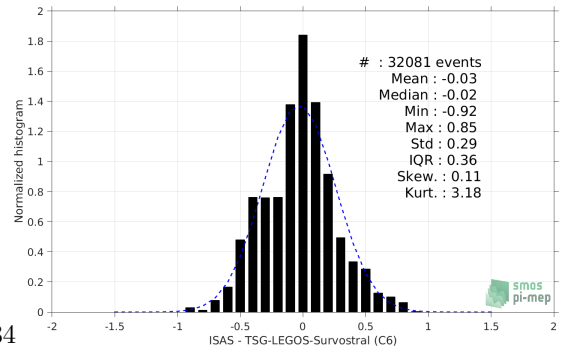

(f) Locations where WOA2013 SSS STD>0.2

Figure 39: Temporal mean (left) and Normalized histogram (right) of ΔSSS (ISAS - TSG-LEGOS-Survostral) for 3 different subdatasets corresponding to C1 (a,b), C2 (c,d) and C6 (e,f).

2.6 TSG-LEGOS-Survostral-Adelie

2.6.1 Number of SSS data as a function of time and distance to coast

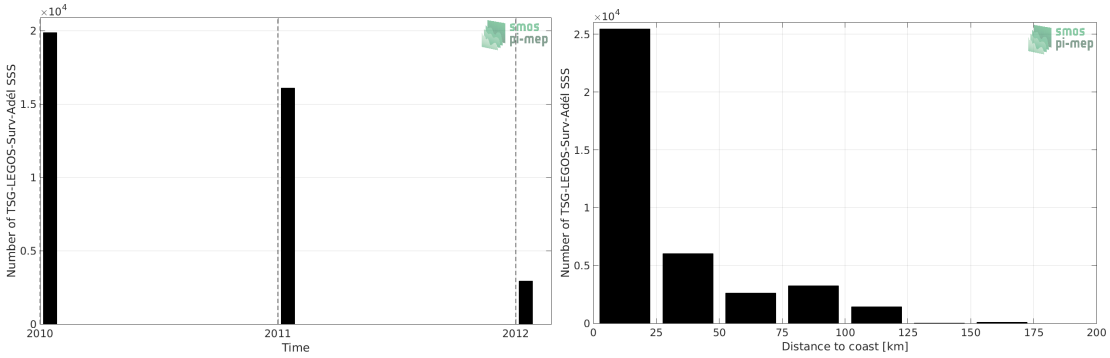

Figure 40: Number of SSS from TSG-LEGOS-Surv-Adel) as a function of time (left) and distance to coast (right).

2.6.2 Histogram of SSS

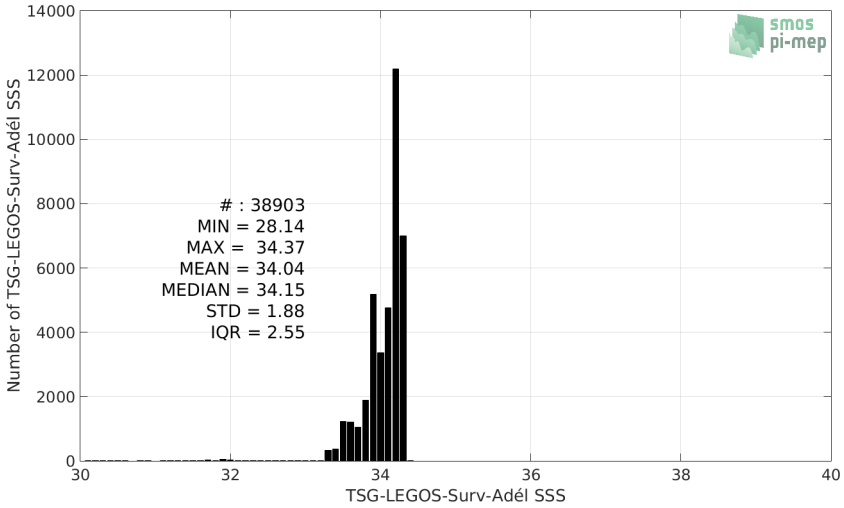

Figure 41: Distribution of SSS from TSG-LEGOS-Surv-Adel) per bins of 0.1.

2.6.3 Temporal mean of SSS

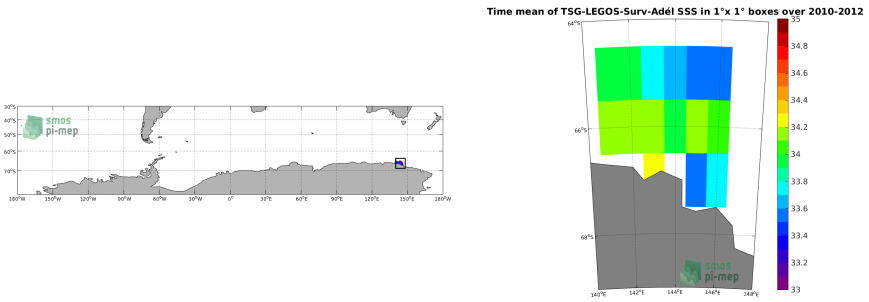

Figure 42: Time-mean SSS from TSG-LEGOS-Surv-Adel) in 1°x1° boxes.

2.6.4 Temporal STD of SSS

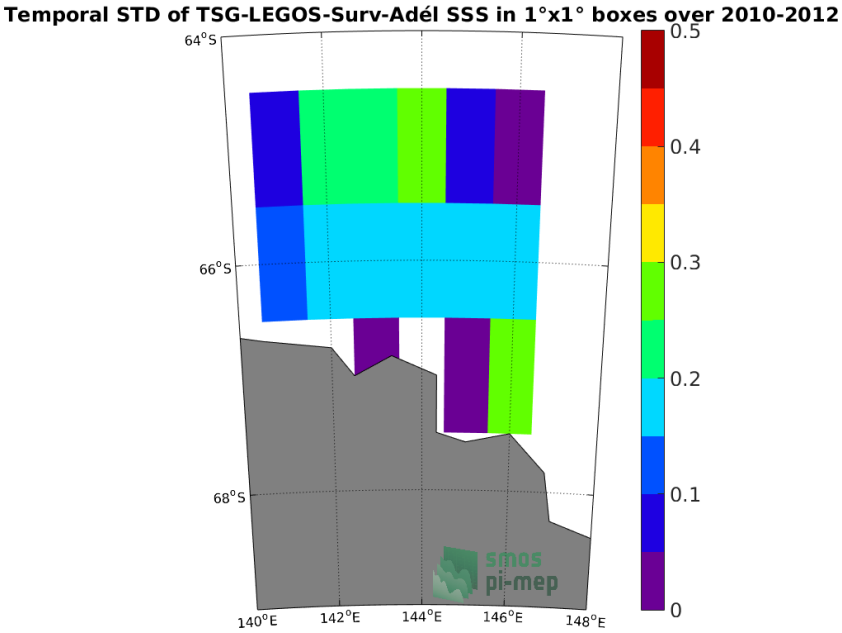

Figure 43: Temporal STD of SSS from TSG-LEGOS-Surv-Adel) in 1°x1° boxes.

2.6.5 Spatial density of SSS

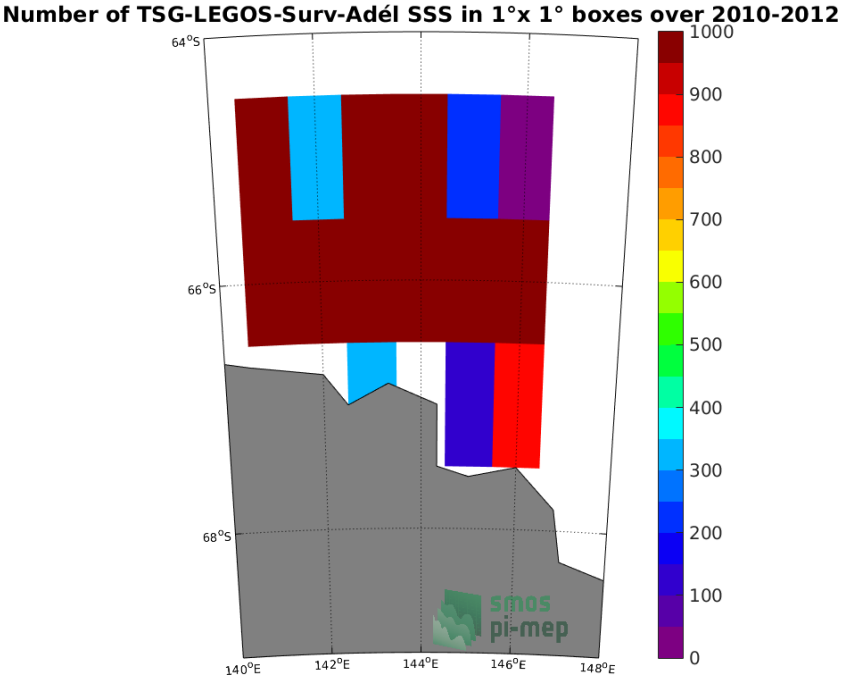

Figure 44: Number of SSS from TSG-LEGOS-Surv-Adel) in 1°x1° boxes.

2.6.6 ΔSSS sorted as geophysical conditions

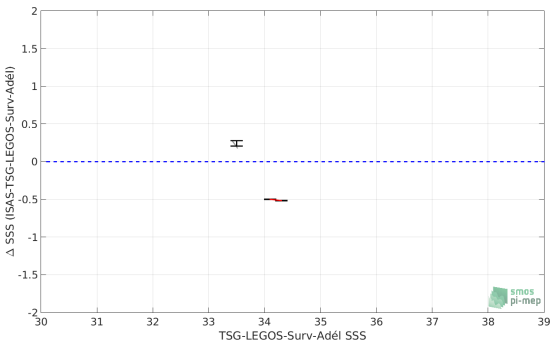

(a) TSG-LEGOS-Surv-Adel) SSS

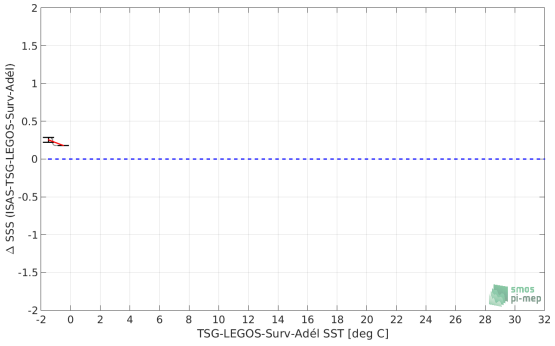

(b) TSG-LEGOS-Surv-Adel) SST

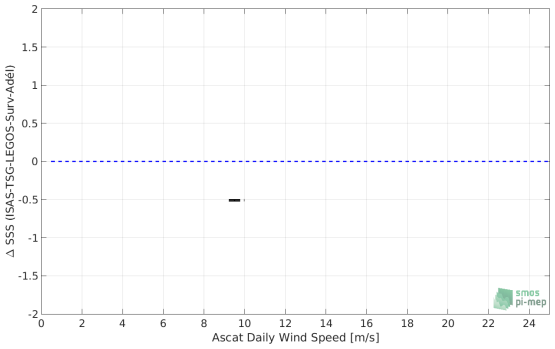

(c) ASCAT Wind Speed

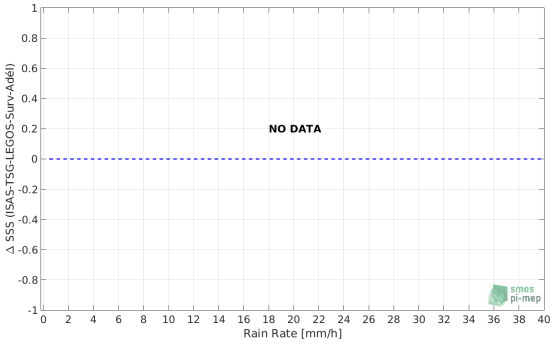

(d) CMORPH Rain rate

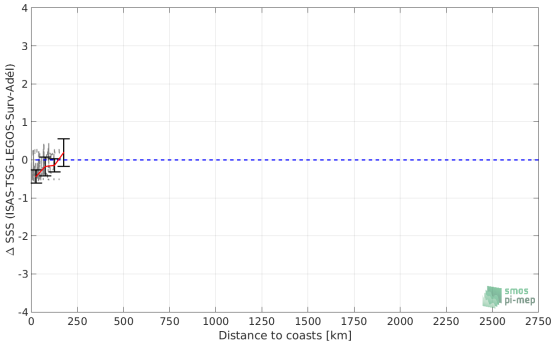

(e) Distance to coast

Figure 45: Δ SSS (ISAS - TSG-LEGOS-Surv-Adel)) sorted as geophysical conditions: TSG-LEGOS-Surv-Adel) SSS a), TSG-LEGOS-Surv-Adel) SST b), ASCAT Wind speed c), CMORPH rain rate d) and distance to coast (e).

2.6.7 Conditional analyses

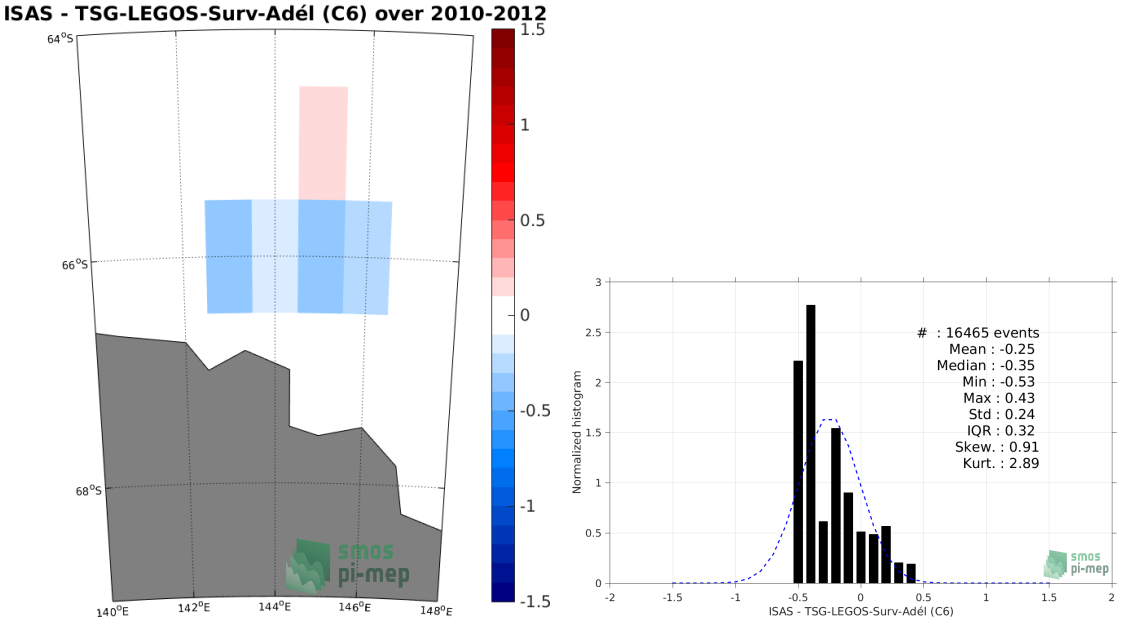

(a) Locations where WOA2013 SSS STD>0.2 (b) Locations where WOA2013 SSS STD>0.2

Figure 46: Temporal mean (a) and normalized histogram (b) of ΔSSS (ISAS - TSG-LEGOS-Surv-Adel)) for 1 subdataset corresponding to C6.

3 Summary

3.1 Number of SSS data as a function of time

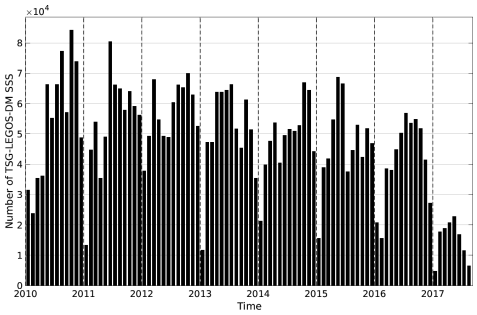

(a) TSG-LEGOS-DM

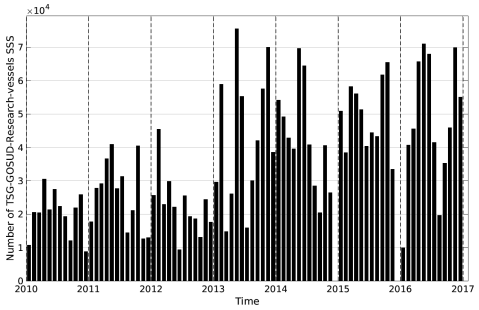

(b) TSG-GOSUD-Research-vessel

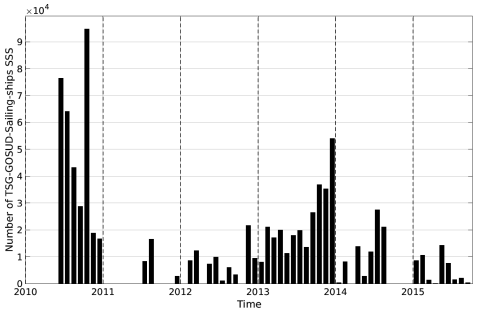

(c) TSG-GOSUD-Sailing-ship

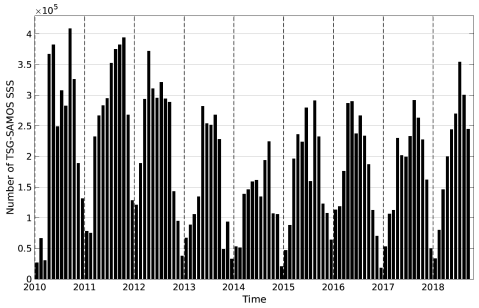

(d) TSG-SAMOS

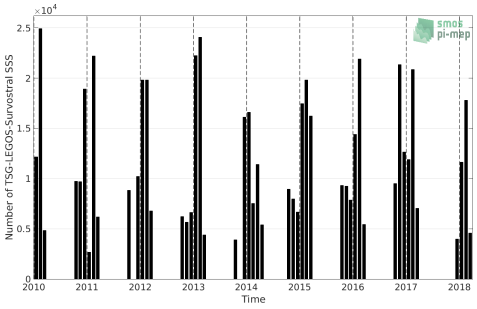

(e) TSG-LEGOS-Survostral

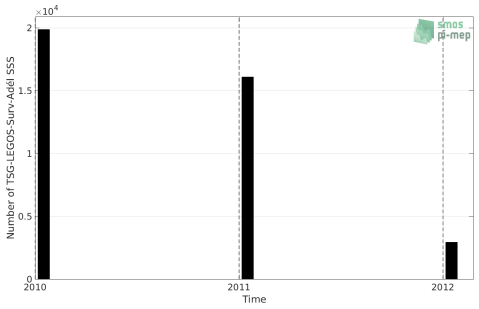

(f) TSG-LEGOS-Survostral-Adélie

Figure 47: Number of SSS data as a function of time.

3.2 Histogram of SSS

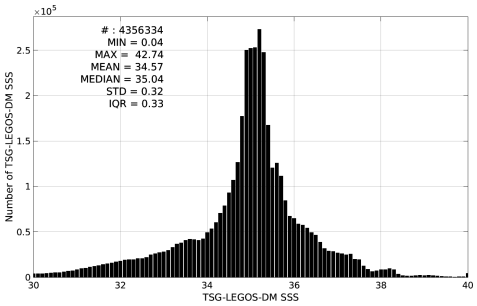

(a) TSG-LEGOS-DM

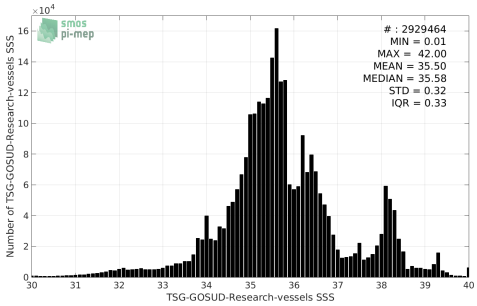

(b) TSG-GOSUD-Research-vessel

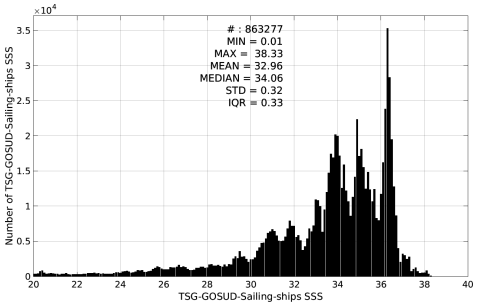

(c) TSG-GOSUD-Sailing-ship

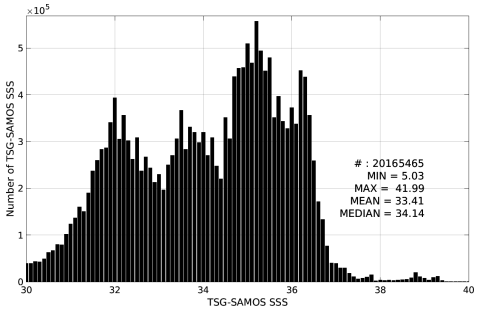

(d) TSG-SAMOS

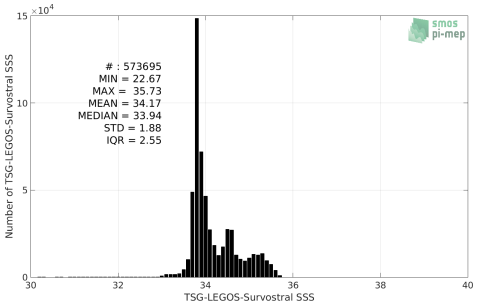

(e) TSG-LEGOS-Survostral

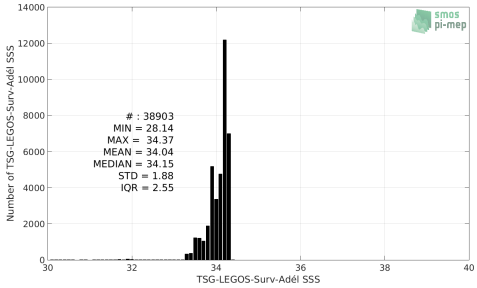

(f) TSG-LEGOS-Survostral-Adélie

Figure 48: Distribution of SSS per bins of 0.1.

3.3 Temporal mean of SSS

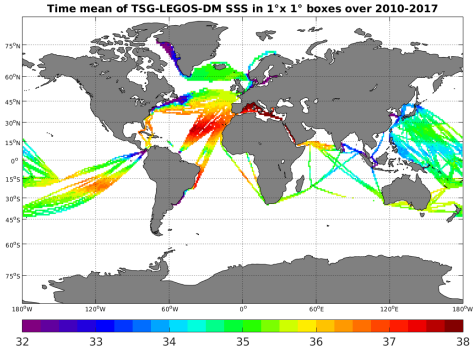

(a) TSG-LEGOS-DM

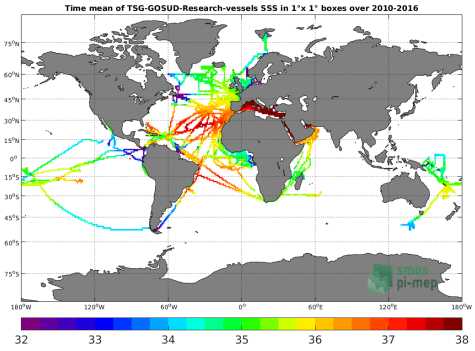

(b) TSG-GOSUD-Research-vessel

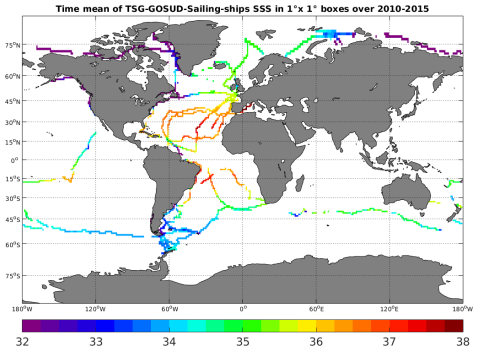

(c) TSG-GOSUD-Sailing-ship

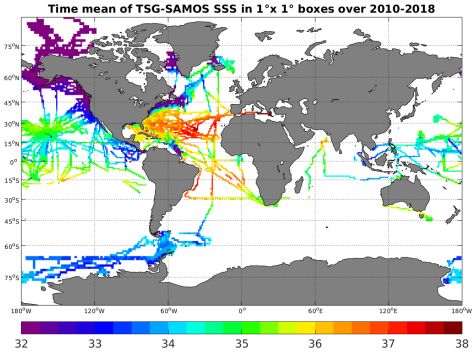

(d) TSG-SAMOS

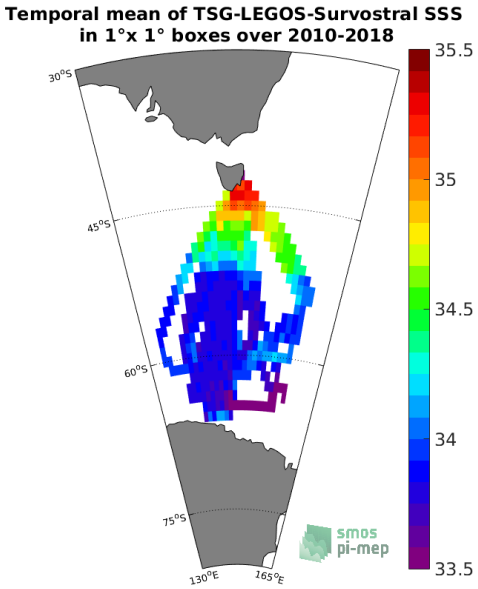

(e) TSG-LEGOS-Survostral

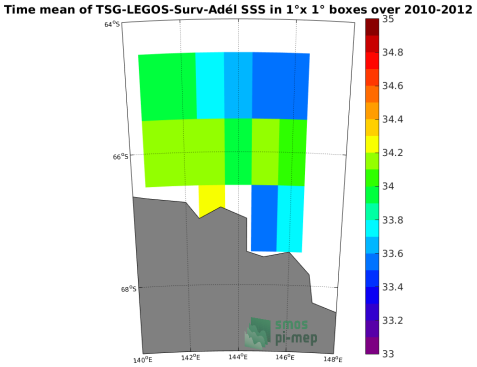

(f) TSG-LEGOS-Survostral-Adélie

Figure 49: Temporal mean of SSS in 1°x1° boxes.

3.4 Temporal STD of SSS

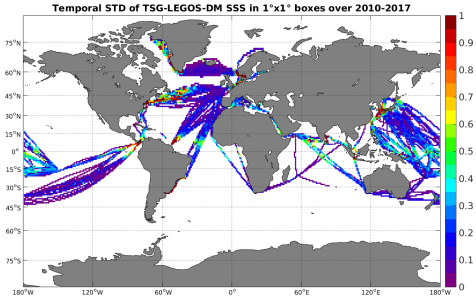

(a) TSG-LEGOS-DM

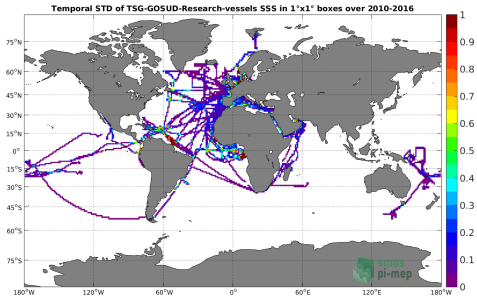

(b) TSG-GOSUD-Research-vessel

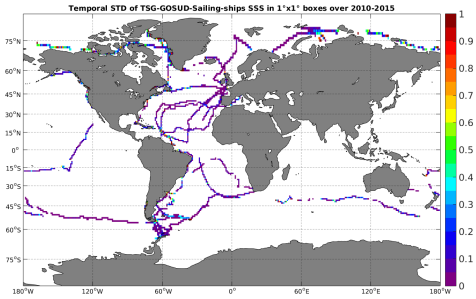

(c) TSG-GOSUD-Sailing-ship

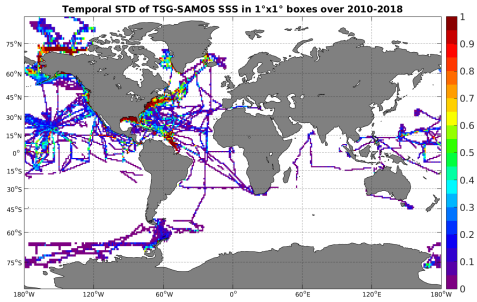

(d) TSG-SAMOS

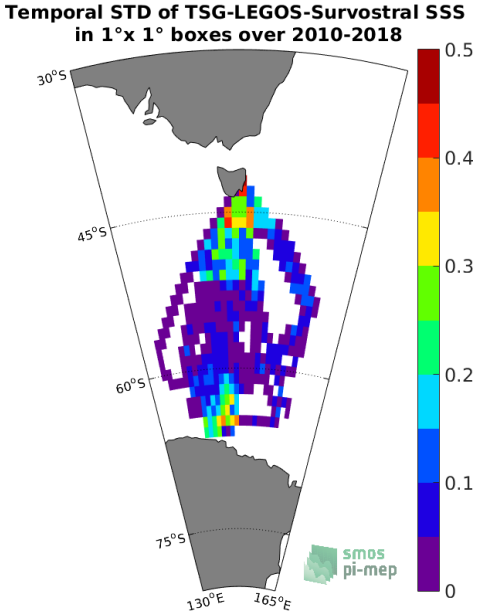

(e) TSG-LEGOS-Survostral

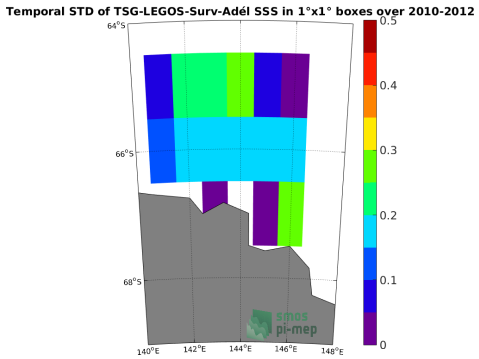

(f) TSG-LEGOS-Survostral-Adélie

Figure 50: Temporal STD of SSS in 1°x1° boxes.

3.5 Spatial density of SSS

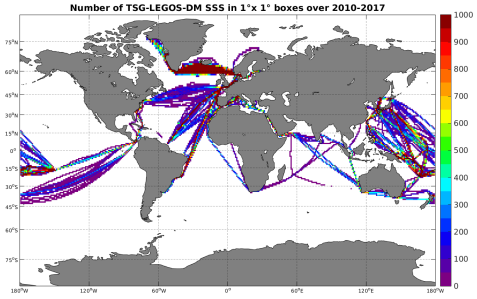

(a) TSG-LEGOS-DM

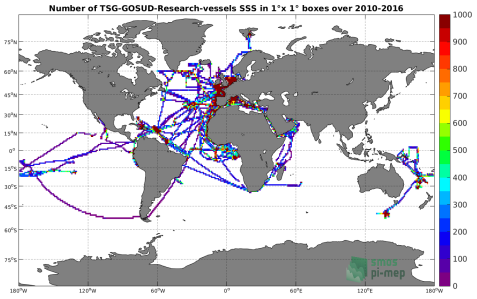

(b) TSG-GOSUD-Research-vessel

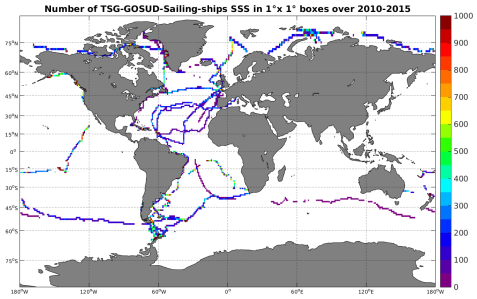

(c) TSG-GOSUD-Sailing-ship

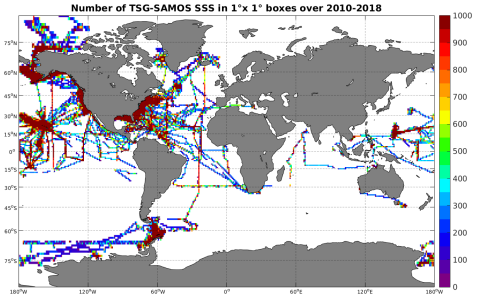

(d) TSG-SAMOS

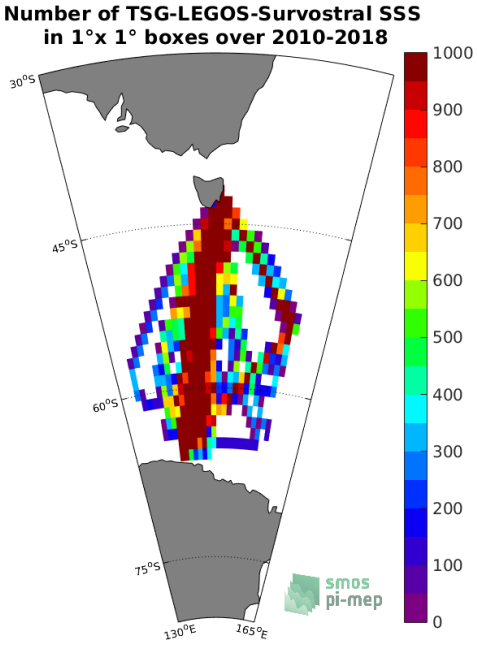

(e) TSG-LEGOS-Survostral

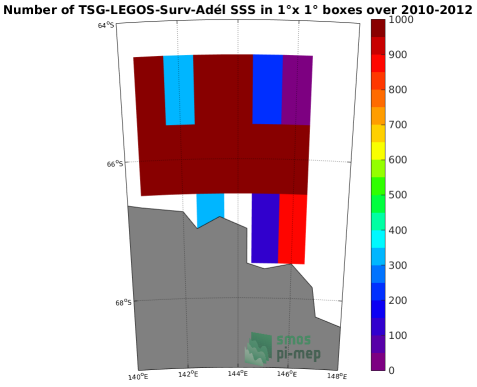

(f) TSG-LEGOS-Survostral-Adélie

Figure 51: Number of SSS in 1°x1° boxes.

References

Gaël Alory, T. Delcroix, P. Téchiné, D. Diverrès, D. Varillon, S. Cravatte, Y. Gouriou, J. Grelet, S. Jacquin, E. Kestenare, and et al. The French contribution to the voluntary observing ships network of sea surface salinity. *Deep-Sea Res. Pt. I*, 105:1–18, November 2015. ISSN 0967-0637. doi: 10.1016/j.dsr.2015.08.005.

Abderrahim Bentamy and Denis Croize Fillon. Gridded surface wind fields from Metop/ASCAT measurements. *Int. J. Remote Sens.*, 33(6):1729–1754, March 2012. ISSN 1366-5901. doi: 10.1080/01431161.2011.600348.

Abderrahim Bentamy, Semyon A. Grodsky, James A. Carton, Denis Croizé-Fillon, and Bertrand Chapron. Matching ASCAT and QuikSCAT winds. *J. Geophys. Res.*, 117(C2), February 2012. ISSN 0148-0227. doi: 10.1029/2011JC007479. C02011.

Jaqueline Boutin, Y. Chao, W. E. Asher, T. Delcroix, R. Drucker, K. Drushka, N. Kolodziejczyk, T. Lee, N. Reul, G. Reverdin, J. Schanze, A. Soloviev, L. Yu, J. Anderson, L. Brucker, E. Dinnat, A. S. Garcia, W. L. Jones, C. Maes, T. Meissner, W. Tang, N. Vinogradova, and B. Ward. Satellite and In Situ Salinity: Understanding Near-Surface Stratification and Sub-footprint Variability. *Bull. Am. Meterol. Soc.*, 97(8):1391–1407, 2016. ISSN 1520-0477. doi: 10.1175/bams-d-15-00032.1.

Ralph R. Ferraro. Ssm/i derived global rainfall estimates for climatological applications. *J. Geophys. Res.*, 1021:16715–16736, 07 1997. doi: 10.1029/97JD01210.

Ralph R. Ferraro, Fuzhong Weng, Norman C. Grody, and Limin Zhao. Precipitation characteristics over land from the NOAA-15 AMSU sensor. *Geophys. Res. Lett.*, 27(17):2669–2672, 2000. doi: 10.1029/2000GL011665.

Fabienne Gaillard, E. Autret, V. Thierry, P. Galaup, C. Coatanoan, and T. Loubrieu. Quality Control of Large Argo Datasets. *J. Atmos. Oceanic Technol.*, 26(2):337–351, 2012/10/10 2009. doi: 10.1175/2008JTECHO552.1.

Fabienne Gaillard, Denis Diverres, Stéphane Jacquin, Yves Gouriou, Jacques Grelet, Marc Le Menn, Joelle Tassel, and Gilles Reverdin. Sea surface temperature and salinity from French research vessels, 2001-2013. *Sci. Data*, 2(150054), October 2015. ISSN 2052-4463. doi: 10.1038/sdata.2015.54.

Fabienne Gaillard, Thierry Reynaud, Virginie Thierry, Nicolas Kolodziejczyk, and Karina von Schuckmann. In Situ-Based Reanalysis of the Global Ocean Temperature and Salinity with ISAS: Variability of the Heat Content and Steric Height. *J. Clim.*, 29(4):1305–1323, February 2016. ISSN 1520-0442. doi: 10.1175/jcli-d-15-0028.1.

Robert J. Joyce, John E. Janowiak, Phillip A. Arkin, and Pingping Xie. CMORPH: A Method that Produces Global Precipitation Estimates from Passive Microwave and Infrared Data at High Spatial and Temporal Resolution. *J. Hydrometeorol.*, 5(3):487–503, June 2004. ISSN 1525-7541. doi: 10.1175/1525-7541(2004)005⟨0487:camtpg⟩2.0.co;2.

Nicolas Kolodziejczyk, Gilles Reverdin, and Alban Lazar. Interannual Variability of the Mixed Layer Winter Convection and Spice Injection in the Eastern Subtropical North Atlantic. *J. Phys. Oceanogr.*, 45(2):504–525, Feb 2015. ISSN 1520-0485. doi: 10.1175/jpo-d-14-0042.1.

Christian Kummerow, Y. Hong, W. S. Olson, S. Yang, R. F. Adler, J. McCollum, R. Ferraro, G. Petty, D-B. Shin, and T. T. Wilheit. The Evolution of the Goddard Profiling Algorithm (GPROF) for Rainfall Estimation from Passive Microwave Sensors. *J. Appl. Meteorol.*, 40(11): 1801–1820, 2001. doi: 10.1175/1520-0450(2001)040⟨1801:TEOTGP⟩2.0.CO;2.

Rosemary Morrow and Elodie Kestenare. Nineteen-year changes in surface salinity in the southern ocean south of australia. *J. Mar. Sys.*, 129:472–483, January 2014. doi: 10.1016/j.jmarsys.2013.09.011.

Thierry Reynaud, Floriane Desprez De Gesincourt, Fabienne Gaillard, Hervé Le Goff, and Gilles Reverdin. Sea Surface Salinity from Sailing ships : Delayed mode dataset, annual release, 2015. doi: 10.17882/39476.

Shawn R. Smith, Jeremy J. Rolph, Kristen Briggs, and Mark A. Bourassa. Quality-Controlled Underway Oceanographic and Meteorological Data from the Center for Ocean-Atmospheric Predictions Center (COAPS) - Shipboard Automated Meteorological and Oceanographic System (SAMOS), 2009. doi: 10.7289/v5qj7f8r.